Creating an Urban Heat Vulnerability Index (HVI) in the Face of Climate Change

Employing Geospatial Technology in Halifax, Canada

By
Md Mehedi Hasan

A Thesis Submitted to
Saint Mary's University, Halifax, Nova Scotia
in Partial Fulfillment of the Requirements for
the Degree of Master of Arts in Geography

March, 2024, Halifax, Nova Scotia

Approved: Dr. Khan R Rahaman
(Co-Supervisor)

Approved: Dr. Mathew Novak
(Co-Supervisor)

Approved: Dr. Peter Bush
(Committee Member)

Approved: Dr. MD Jahedul Alam
(External Examiner)

Date: March 25, 2024

Creating an Urban Heat Vulnerability Index (HVI) in the Face of Climate Change Employing Geospatial Technology in Halifax, Canada

By Md Mehedi Hasan

Abstract

Heat waves are one of the most common weather events happening in recent decades, posing threats to public health especially in urban built-up environments. This study employs geospatial techniques to evaluate urban heat vulnerability in the city of Halifax, Nova Scotia, Canada. The Heat Vulnerability Index (HVI) was developed through the utilization of the Geographic Information System (GIS), integrating exposure, sensitivity, and adaptive capacity measures generated using Remote Sensing (GIS) and socio-economic datasets for four years covering: 2006, 2011, 2016, 2021. The process applies an Equal Weight Approach (EWA) to assign equal importance to the 16 normalized variables considered in creating the comprehensive HVI. The overarching goal of this study was to assess heat vulnerability at a local level by offering a detailed analysis of these 16 proposed indicators in an urban setting. The results revealed that the HVI attained its peak in the year 2021, exhibiting a variable trajectory in its scores, with all years demonstrating a significant high-risk zone encompassing the regional center. Findings may enable multiple stakeholders to understand spatial variability of temperature anomalies at local level and may identify vulnerable populations at risks.

March 25, 2024

Acknowledgments

The realization of this thesis owes a debt of gratitude to numerous individuals whose guidance and support were indispensable. Foremost, I express my deepest appreciation to Dr. Khan Rubayet Rahaman and Dr. Mathew Novak for their generous sharing of knowledge and unwavering patience throughout this journey. Their mentorship has been instrumental in fostering my understanding and growth in the realm of Heat Vulnerability Indexing.

I extend heartfelt thanks to my committee member, Dr. Peter Bush, for ensuring that my defense was not only a scholarly endeavor but also an enjoyable experience, enriched by his insightful comments and suggestions. I am also indebted to the faculty members of the Geography and Environmental Studies Department at Saint Mary's University for their contributions in shaping my academic trajectory.

Beyond the academic realm, I am immensely grateful for the unwavering support of my family, particularly my wife, Rokaiya Akter, whose encouragement and understanding of the time commitments involved were pivotal in my success. I also extend my gratitude to my entire family for their enduring support and understanding throughout the research and writing process. Their prayers have been a source of strength and motivation. A special acknowledgment is reserved for my uncle, Md Israfil Hossain, whose unwavering support during both my undergraduate and graduate studies has been invaluable. His investment in my education is deeply appreciated and has been a cornerstone of my academic journey.

Table of Contents

List of Figures

List of Tables

Chapter 1: Introduction

In response to changing climates, heat vulnerability indexing is increasingly important in fields of urban management and public health. A Heat Vulnerability Index (HVI) delineates neighborhoods in which inhabitants face an elevated risk of mortality during and in the immediate aftermath of extreme heat events. Employing a statistical model, the index synthesizes key social and environmental determinants contributing to the vulnerability of a given neighborhood to heat-related risks.

The impact of heat stress varies across Canada due to local climate dynamics, population density, and social factors. This escalation in temperature heightens the risk of adverse effects on agriculture, water resources, droughts, and public health. Extreme high temperatures pose significant hazards to human health, with increased risks of illness and mortality, especially in tropical regions where higher temperatures and humidity levels coincide more frequently. Climate and weather factors such as temperature, humidity, precipitation, and wind speed significantly influence forest fire danger.

Extreme high temperatures cause significant health risks, especially in densely populated areas. As temperatures rise, so does the frequency of dangerous heat levels, which can exacerbate existing health issues and strain public resources. In Canada, as in other regions, vulnerable populations, including the elderly and those with pre-existing health conditions, are at increased risk during heatwaves (Sun et al., 2019). Additionally, Indigenous communities, particularly those in remote regions, may face unique challenges in adapting to and mitigating the impacts of heat stress. Efforts to combat heat

stress in Canada must consider the spatial variability of climate impacts and prioritize measures to protect vulnerable populations.

Between 1948 and 2016, there was an elevation of 0.7ºC in the annual mean temperature across Atlantic Canada, accompanied by an 11% augmentation in normalized annual precipitation (Cohen et al., 2019). In contrast to various other Canadian regions, the warming trend observed in Atlantic Canada is primarily attributable to heightened summer temperatures rather than an escalation in winter temperatures, (Cohen et al., 2019) . The ramifications of climate change manifest not only through the gradual shifts in mean temperature and precipitation but also through alterations in climatic extremes. The geographical and climatic complexity of Atlantic Canada, coupled with the anticipated escalation of extreme weather events, poses multifaceted challenges to human health.(Cohen et al., 2019; Dietz & Arnold, 2021; Philippe Roy & David Huard, 2016). Notably, Atlantic Canada's demographic landscape is characterized by an aging population, with projections indicating that by the year 2038, an estimated 31.1% of the total population will be aged 65 years and above (Dietz & Arnold, 2021). This demographic characteristic underscores an augmented susceptibility among elderly individuals to health impacts associated with heightened temperatures. This proportion surpasses the national average of 25.5% (Dietz & Arnold, 2021; Statistics Canada, 2023).

A considerable segment of the outdoor workforce, predominantly comprising males, is involved in the sectors of agriculture, fisheries, forestry, and mining, encompassing 14% of the regional labor force, according to Statistics Canada (2020b). Notably, the mortality

rate for males at the age of 65 is twice that of females, and their mortality rates progressively converge with those of females around the age of 97 (Robine et al., 2012).

Factors contributing to heightened vulnerability in the region include increased built-up area, less canopy cover, high population density, a homeless population, inadequately insulated homes prevalent in older communities, and aging community infrastructure that is more prone to disruption or damage during extreme heat events. These issues are underscored in research by Comeau and Nunes (2019) and are further discussed in the Rural and Remote Communities chapter as well as the Cities and Towns chapter of the National Issues Report.

Temperature, despite being an objective metric, is subjectively felt. Variables like humidity and wind chill are crucial in explaining why identical temperatures can evoke distinct sensations across different regions globally. In warmer areas like southern Ontario, a heat advisory is declared following at least two consecutive days with temperatures at or above 30°C and a humidex of 40°C or higher. In contrast, in Labrador, a heat advisory may be issued after just an hour of the humidex reaching 40°C (Canadian Red Cross, 2024). Whereas the UAE experiences a typical mean temperature range of 32°C to 37°C during the summer months that is normal in that locality (World Bank, 2024). Cultural influences also significantly impact thermal perceptions. As noted by Naheed and Shooshtarian (2021), one's cultural background contributes to variations in thermal tolerance, comfort preferences, clothing choices, environmental attitudes, and overall thermal expectations. Different cultural groups develop varying levels of

tolerance and comfort perceptions in response to thermal conditions(Naheed & Shooshtarian, 2021).

Our bodies strive to maintain a steady internal temperature of 37°C under normal circumstances (CCOHS, 2024). When it's hot, we sweat to cool down through evaporation. However, higher humidity levels hinder evaporation, leading to a rise in body temperature and potential health risks, especially when relative humidity hits around 90 percent (CCOHS, 2024). Likewise, wind can swiftly steal our body's heat, creating a sensation of temperatures several degrees lower than the actual temperatures. Thermal comfort metrics are not universally standardized; different countries employ diverse methods of gauging how hot a day feels, influencing risk communication and comprehension. For example, Canada uses "Humidex" to quantify perceived heat (CCOHS, 2024), while the USA relies on "Heat Index" to assess the apparent temperature, considering both air temperature and relative humidity (NOAA, 2024). Additionally, there's the "WBGT" (wet bulb globe temperature) system that evaluates heat stress during outdoor activities, factoring in temperature, humidity, wind speed, sun angle, and cloud cover. This method is utilized by military agencies, the Occupational Safety and Health Administration, sports associations, and others to regulate workload or exertion levels (NOAA, 2024). Moreover, various entities have proprietary versions with undisclosed formulas, such as AccuWeather's "RealFeel," contributing further complexity to understanding and managing heat-related risks.

This study dealt with LST based heat vulnerability indexing. Producing an HVI is an essential tool as it demonstrates the spatial distribution of heat vulnerability across a region factoring in vulnerable communities in the analysis. With a HVI in place, governments can identify areas of concern and target interventions to enhance public health infrastructure, implementing urban greening initiatives to mitigate the urban heat island effect, and improving emergency response systems to effectively address heat-related emergencies. Moreover, investments in sustainable land management and climate-resilient infrastructure can help mitigate the risk of wildfires and reduce their impact on communities and ecosystems.

The principal aim of this research is to assess the prospective susceptibility to LST based heat-related challenges within the urbanized areas of the Halifax Regional Municipality (HRM), Nova Scotia. This was accomplished through the application of a rigorous methodological framework based on established practices in producing HVI and spanning four distinct census years, specifically 2006, 2011, 2016, and 2021. The study encompassed two primary procedures: (i) creating indexes on land-surface temperature, heat sensitivity, and adaptive capacity and (ii) merging these three vulnerability assessment methods to create a HVI. To enhance comprehension and corroborate the findings of the HVI, indices for Urban Heat Island (UHI) were generated. Once created, the UHI helped to identify areas within Halifax that experience higher temperatures due to urbanization and human activities, highlighting areas that experience significantly higher temperatures compared to their surroundings. Adding UHI mapping allows for a deeper understanding of which populations are most at risk and why, corroborating the

results of the original HVI, and ensuring targeted interventions and resources are suitably allocated.

This research is structured into six chapters, commencing with an extensive literature review in chapter two that elucidates seminal investigations pertaining to Heat Vulnerability Indexing. Chapter three expounds upon the methodologies employed, encompassing both the delineation of the study area and the acquisition of datasets. The study confines its scope to the urban precinct of Halifax, Canada. Socioeconomic data boundary shapefiles utilized in this research were procured from the Statistics Canada website while spatial data, including Landsat 5 & 8 from the USGS website and Landcover Data from the Commission for Environmental Cooperation of North America's website, were instrumental. The analysis is executed at the level of Census Dissemination Areas (DAs). Chapter four meticulously presents the outcomes derived from the analytical procedures. Subsequently, chapter five provides a comprehensive discussion, affording an opportunity to delve into the findings expounded in chapter four. The concluding chapter culminates the study by accentuating key insights gleaned from the research, proffering recommendations for future research trajectories, and deliberating on the ramifications of the research findings vis-à-vis practical policy enhancements.

Chapter 2: Literature Review

Contemporary climate projections clearly indicate that the effects of greenhouse gas emissions are fueling climate change with escalating temperatures across many urbanized areas throughout the 21st century (IPCC, 2013; Meehl & Tebaldi, 2004; Schär et al., 2004). Numerous global and regional studies have underscored the heightened likelihood of heatwaves as an expected consequence(Beniston et al., 2007; Chauvin & Denvil, 2007; Huth et al., 2000; Vautard et al., 2007). In 2019, the average temperature has approached nearly 1 degree Celsius above the 20th-century average of 13.9°C, as reported by the National Oceanic and Atmospheric Administration (NOAA) (NOAA, 2023). Additionally, the years from 2015 to 2019 were characterized by some of the most lethal heatwaves, as documented by the World Meteorological Organization (WMO) (WMO, 2019). Across the globe, cities are increasingly experiencing unpleasant and life-threatening situations due to exceptionally high temperatures (Brooke Anderson & Bell, 2011; Geladi, 2018; Harlan et al., 2013; Loughnan et al., 2013; Sheridan et al., 2012). And there is a growing apprehension between both the public and institutional stakeholders regarding the increased vulnerability of urban areas to these occurrences (Lemonsu et al., 2015).

The twenty-first century is expected to witness an escalation in the frequency, severity, and duration of the extreme heat events across North America and Europe with potential exacerbation due to elevated humidity and increased levels of air pollution (Kershaw & Millward, 2012). Extreme heat events currently stand as the leading cause of summer-related fatalities in the United States, emphasizing the critical need for research in heat

risk assessment. According to the World Health Organization (WHO), heatwaves accounted for more than 166,000 fatalities between 2000 and 2017 (Karanja & Kiage, 2021; United States Environmental Protection Agency Office of Atmospheric Programs, 2006). The severe heatwaves of 2003, which claimed more than 15,000 lives in France and 30,000 across all of Europe (Karanja & Kiage, 2021; United States Environmental Protection Agency Office of Atmospheric Programs, 2006). Canadian cities have also experienced excessive mortality rates due to extreme heat events (Aminipouri et al., 2016). From 1900 to 2009, Canada has documented six such extreme heat events, which collectively led to a little over 1,300 fatalities (as reported by Public Safety Canada in 2013 and Health Canada in 2011) (Government of Canada, 2014; Health Canada, 2011). In Vancouver, the extreme heat event of the summer of 2009 was associated with an estimated excess mortality of 112 individuals (Aminipouri et al., 2016).

According to Health Canada, common high-risk demographics encompass seniors, young children, individuals with chronic illnesses, and those who are socially disadvantaged, while the outcomes may differ based on specific locations and events (Harlan et al., 2013; Health Canada, 2011; Hondula et al., 2015). In late July and early August 2009, Vancouver International Airport has recorded a maximum and minimum temperatures of 30.9°C (19.6°C) on July 28, 34.0°C (20.2°C) on July 29, and 34.4°C (22.4°C) on July 30, all under clear skies with an average relative humidity of 57% (Baccini et al., 2011). Shortly after the onset of the heatwave, BC's rapid mortality surveillance system has revealed a 40% increase in deaths among greater Vancouver residents through August 2009 (Baccini et al., 2011). The stagnant atmospheric conditions and the unrelenting solar

radiation have also contributed to the accumulation of high ground-level ozone concentrations, prompting the region to be placed under an air quality advisory for most of the heat dome's duration in 2021 in BC (Henderson et al., 2021). According to (Health Canada, 2023), Nova Scotia has been identified as one of the regions expected to experience a rise in extreme heat events, which pose significant risks to the health and well-being of the local communities (Health Canada & Government of Canada, 2023). The forecast indicates that Nova Scotia is likely to witness an annual increase in the number of hot days, with some areas, such as Annapolis County, possibly encountering 6-10 days where temperatures exceed 30°C by the year 2050 (Health Canada & Government of Canada, 2023). Health Canada has also recognized that extreme temperatures pose a heightened risk, especially for young children, pregnant women, older adults, individuals with chronic health conditions, and those who engage in outdoor work or exercise (Health Canada & Government of Canada, 2023). To address these concerns, a collaborative effort involving Environment and Climate Change Canada, Health Canada, and the Nova Scotia Department of Health and Wellness has been established to implement a heat alert system in 2023 (Health Canada & Government of Canada, 2023).

In light of these temperature increases, the concept of Urban Heat Island (UHI) has become a critical area of research in the recent urban climate literature and significantly impacting the urban built environment(Leya et al., 2022). UHI relies on several factors related to spatial dimensions, configuration, composition, landscapes, and layout of city’s neighborhoods while delineating the surface temperature. The UHI effect is a heat

accumulation phenomenon that occurs within urban areas because of urban development and human activities (Yang et al., 2016).

The HVI enables a more comprehensive examination of heat-related risk factors, aiding multiple stakeholders in making efficient decisions for areas with comparatively greater heat vulnerability(Mallen et al., 2019). Heat-related morbidity and mortality among vulnerable populations may rise with the projected increase in frequency, intensity, and the duration of extreme heat events worldwide(Nayak et al., 2018). Implementing HVI assessments at the neighborhood level may empower public health professionals and emergency responders to assist populations facing elevated risks of heat-related stress. The capacity to visually represent the spatial distribution of heat vulnerability at neighborhood scale is in demand and can enable local authorities to allocate resources efficiently and provide aid to the most vulnerable areas. Findings from this research may enable local government organizations to concentrate their emergency response and services and aid the existing climate-adaptation strategies in neighborhoods where the risk of heat-related illnesses and fatalities is evident(Chuang & Gober, 2015).
HVIs serve as a methodology for evaluating heat vulnerability by focusing on three risk components (i.e., Sensitivity, Exposure and Adaptive Capacity). Physical exposure refers to the proximity of a location to environmental hazards like heatwaves or natural disasters. Sensitivity pertains to the inherent characteristics of a population that affect its vulnerability to these hazards. Adaptive capacity represents the community's ability to effectively manage and respond to the consequences and aftermath of hazardous events (Chuang & Gober, 2015).

In the body of literature, several methods have been identified to delineate HVI around the world. Principal Component Analysis (PCA) (Harlan et al., 2013; Hondula et al., 2015; Johnson et al., 2012; Maier et al., 2014; Nayak et al., 2018; Reid et al., 2009; Wolf & McGregor, 2013) is commonly used to reduce multiple heat-related indicators to a smaller set of uncorrelated principal components, which capture most of the variation in the data. EWA (Aubrecht & Özceylan, 2013; W. T. L. L. Chow et al., 2013; X. Liu et al., 2020; Tomlinson et al., 2011a; Vescovi et al., 2005) is used to assign the same proportion to each vulnerability indicator and aggregate them to derive the HVI. Geographic Information System (GIS) (Bradford et al., 2015; Inostroza et al., 2016; Yuan & Bauer, 2007) is used to integrate spatially explicit indicators for exposure, sensitivity, and adaptive capacity within a GIS environment to calculate the HVI. Furthermore, Local Indicators of Spatial Association (LISA) (Corbin, 2015) is used to identify hotspots, cold spots, and outliers in vulnerability within specific geographic regions. Nayak et al., (2018) have conducted a univariate analysis and have evaluated the correlations among the variables using Spearman's correlation coefficients (Nayak et al., 2018). Where the correlation has helped to identify a pattern among the variables. In this method, PCA is used additionally to provide weight to the variables and then reduce the number of variables to a smaller set of principal components. These normalized scores are then divided into six groups based on their mean and standard deviations. Each group is assigned a score ranging from 1 to 6, where a score of 1 represents the least vulnerability, and a score of 6 indicates the highest vulnerability. The HVI is then formulated by summing the scores across the components for every census tract. Mallen et al., (2019) have compared heat vulnerability scores through a PCA to estimate the HVI (Mallen et

al., 2019). Afterwards, they have integrated these obtained scores with heat-related mortality. These analyses have been carried out specifically for the City of Dallas, Texas, USA, utilizing high-resolution land cover datasets (produced based on classified aerial imageries) generously provided by the City of Dallas and the Texas Trees Foundation (Mallen et al., 2019). Liu et al., (2020) have used both (i) EWA and (ii) PCA to identify and summarize indicators for obtaining the HVI (X. Liu et al., 2020). In this study, the authors have used Google Earth Engine (GEE) to retrieve satellite data, which is from Landsat 8 (provided by USGS). While the thermal infrared band of Landsat 8 originally have a spatial resolution of 100 meters, the USGS resamples all its products to 30 meters using a cubic convolution resampling technique. They have employed GEE, and used Landsat 8 surface reflectance tier 1 dataset, which allowed them to compute the average Land Surface Temperature (LST) during the period spanning June to August in 2013 (X. Liu et al., 2020).

In EWA, they have assumed that all nine indicators held equal influence on heat vulnerability. Consequently, they aggregated these indicators with equal weighting to derive the final heat vulnerability metric, denoted as HVIEWA.

In PCA, they have utilized varimax rotation to ensure orthogonality among the reduced indicators, thereby enhancing their ability to transform correlated indicators into linearly uncorrelated components (X. Liu et al., 2020).

Inostroza et al., (2016) have developed the HVI utilizing a Geographic Information System (GIS) to integrate spatially explicit indicators for exposure, sensitivity, and

adaptive capacity. These indicators are derived from both remote sensing data and socio-economic information, are processed through PCA (Inostroza et al., 2016). The HVI is formulated as a function of component impacts and adaptive capacity, which were themselves characterized by exposure and sensitivity. This disaggregated approach allows them to better understand variations in vulnerability levels, compared to a bulk assessment, making it more valuable for informing policy decisions. They conducted a PCA, which statistical technique have transformed the original variables into a smaller number of principal components that capture most of the variance in the observed data. They also used a variance-weighted approach to assign weights to the variables by aggregating the variance explained by each component. They further have enhanced their interpretations and have dispersed loadings across the principal components by applying an orthogonal (Varimax) rotation of eigenvectors. This has resulted in interpretable factors that revealed a simpler structure. The resulting z-score matrix represents a new set of uncorrelated variables, enabling further mathematical analysis (Inostroza et al., 2016). To facilitate this analysis, they have standardized all datasets, transforming them into ratios ranging between zero and one and have created four distinct data matrices, each corresponding to a specific urban type, and accounting for various land type classes. Parallel analysis is conducted on each matrix, suggesting the optimal number of factors required to adequately represent the covariance structure among observed variables. To analyze the spatial distribution of vulnerability across different urban classes in Nebraska, (Corbin, 2015) has employed the Local Indicators of Spatial Association (LISA) methodology. This technique helps identify hotspots, cold spots, and outlier census tracts based on total vulnerability. LISA compares the difference in the desired variable for each

tract with that of its neighboring tracts, using a distribution of permutations with randomly assigned values to the tracts.

Several existing studies focus on the United States and various European cities, with limited research conducted in Canada. Notably, only a few provinces, such as BC and Ontario, have received significant attention from researchers, while others, like Nova Scotia, have added little to no research articles and scientific evidence. Halifax makes for an obvious case for producing a HVI as it serves as the primary city in Nova Scotia and the largest city in Canada's Maritime region. Previous literature highlights the importance of categorizing variables for the development of the HVI; however, most variables used in previous studies are not suitable for this specific study area. Extensive background research determined the appropriate variables for developing the HVI within three major categories: Exposure, Sensitivity, and Adaptive Capacity. Exposure consists of Land Surface Temperature (LST), impervious surfaces, tree cover, population density and daytime population density to identify areas with the greatest exposure to heat stress. Sensitivity considered variables such as the proportion of people over the age of 65, individuals living alone, low-income households, and those with lower levels of education to assess sensitivity. Finally, adaptive capacity considered income, education levels, and access to air conditioning as factors in calculating the adaptive capacity of the population. Each of the variables in the index was assigned an equal weighting (Aubrecht & Özceylan, 2013; W. T. L. Chow et al., 2012; Dong et al., 2014; Tomlinson et al., 2011b). Google Earth Engine (GEE), and data from Landsat 5 and 8 were employed to determine the Land Surface Temperature (LST).

Chapter 3: Methods

3.1 Study Area

Halifax is the primary urban center of Canada's Maritime region and is also the provincial capital of Nova Scotia. The city is situated at 44°52′00″N and 63°42′58″W with an area of approximately 5,475.57 km^2 (i.e., Regional Municipality) (Hasan et al., 2023; Statistics Canada, 2023). A significant consolidation took place in 1996, leading to the formation of HRM by merging the city of Halifax, the city of Dartmouth, the town of Bedford, and Halifax County Municipality(McGillivray, 2019).

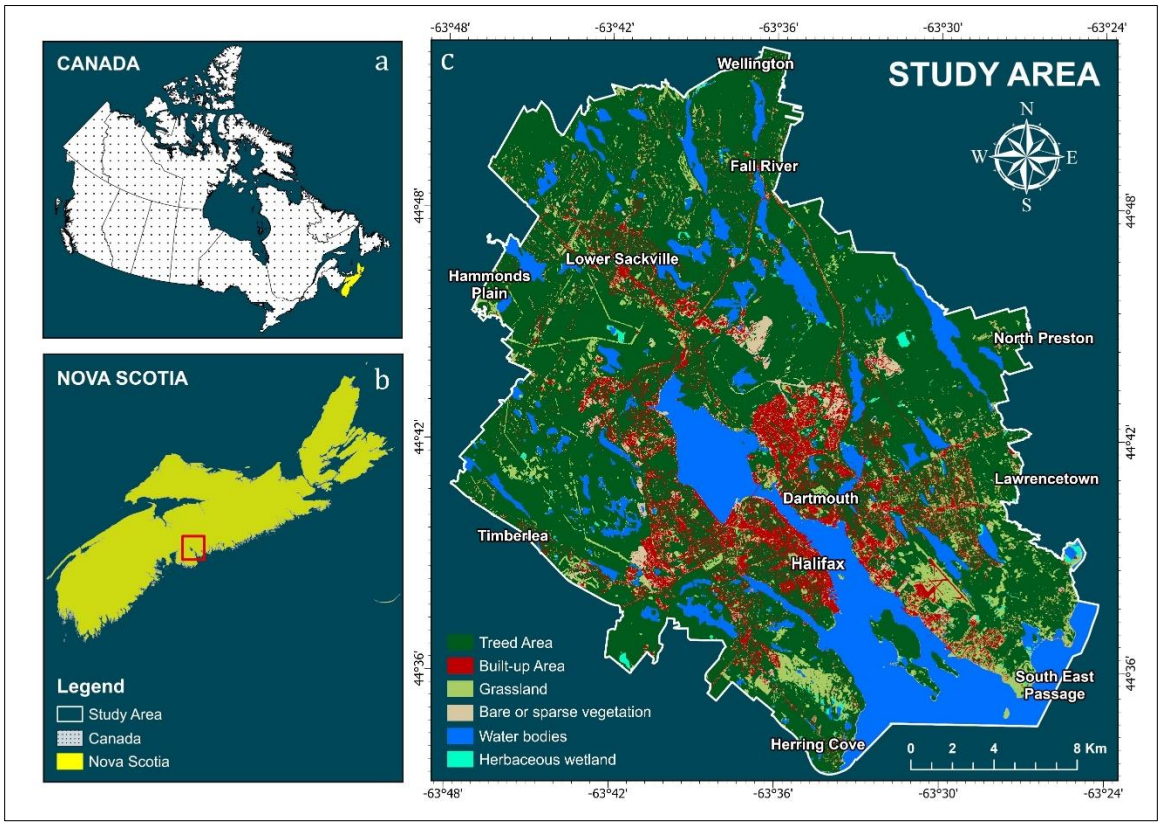

Figure 3.1, (a) Map of Canada showing the location of the province of Nova Scotia. (b) Map of Nova Scotia showing study area location (red box). (c) Study area map showing land cover classes in urban and suburban areas of Halifax. Data Source: Halifax Open Data Portal, World Cover 2021 v200 and GeoNova: Geographic Data Directory.

Halifax experiences a humid continental climate characterized by warm summers and relatively mild winters. January stands as the coldest month, with August being the warmest (Halifax Regional Municipality, n.d.). The highest temperature ever recorded was 37.2 degree Celsius in 1912, while the lowest temperature recorded was -29.4 ˚C in 1922 (Halifax Regional Municipality, n.d.; Kennedy, 2021). The average annual temperature in the HRM area is approximately 7.5˚C, dropping to -5.9 ˚C in the coldest winters and reaching 18.8 ˚C during the warmest summers (Hasan et al., 2023). Precipitation remains high throughout the year (1468.1 mm), and winters see a mix of rain, freezing rain, and snow (154.2 cm). Notably, 2014-15 has been marked as one of the coldest, snowiest, and stormiest periods in the city (Environment and Climate Change Canada., 2023).

In addition to being the provincial capital, Halifax holds the distinction of being the largest municipality and the economic hub of the Atlantic Canada. It hosts over 40% of Nova Scotia's residents, serves as the primary hub for finance, commerce, and industry in both the province and Atlantic Canada (Halifax Regional Municipality, n.d.). The city boasts a wide-ranging manufacturing sector encompassing food processing, furniture production, shipbuilding, clothing manufacturing, and contributions to the aerospace and defense industries (Halifax Regional Municipality, n.d.). It holds the top position in provincial rankings and is the 13th most populous city in the country (Statistics Canada, 2023). From 403,131population in 2016, it has grown by 9.1% to reach 439,819 in 2021. This increase has resulted in a population density of 80.3 people per square kilometer. Between the 2016 and 2021 censuses, Halifax's urban expanse has recorded a 3.57 km^2 increase, transitioning from 234.72 km^2 to 238.29 km^2. Urban expanse occupies a meager

5 percent or less of the municipality's land area (Statistics Canada, 2023). The urban environment is dominated by a few exceptions such as parks and green spaces.

3.2 Variable Selection and Data Requirements:

Extreme heat vulnerability is not uniform across all populations; it varies due to differences in neighborhood socio-economic status, environmental conditions, and infrastructure. Numerous studies have identified a spectrum of factors that impact an individual's or a community's susceptibility to extreme heat events. These factors encompass but are not limited to, local climatic conditions, age, income levels, housing quality, health status, access to cooling facilities, and social support networks (Bélanger et al., 2015; Coates et al., 2014; Gronlund et al., 2015; Harlan et al., 2013; Hondula et al., 2015; Onozuka & Hagihara, 2015; Student et al., 2011).

Table 3.1, Variables identified in previous research.

Title	Author Sources	Variables
A Heat Vulnerability Index: Spatial Patterns of Exposure, Sensitivity and Adaptive Capacity for Santiago de Chile.	(Inostroza et al., 2016)	Exposure: Land Surface Temperature (LST) Sensitivity: i) Elderly population ii) Very young population iii) Disabled population iv) Family structure v) Education level vi) Unemployment Adaptive Capacity: i) Access to communication technologies ii) Access to water supply iii) Material Index iv) Access to medical services v) Normalized Difference Vegetation Index (NDVI) vi) Roads
Development of a heat vulnerability index for New York State.	(Nayak et al., 2018)	i) Social/language vulnerability ii) Socioeconomic vulnerability iii) Environmental/urban vulnerability and

		iv) Elderly/ social isolation.
A methodological assessment of extreme heat mortality modeling and heat vulnerability mapping in Dallas, Texas.	(Mallen et al., 2019)	Exposure: No green space Sensitivity: i) Over age 65 ii) Living alone iii) Over age 65 and living alone iv) Race other than white. Adaptive capacity: i) Living below poverty line ii) Less than high school education iii) No AC access. iv) Diabetes prevalence No full AC access
Mapping Urban Heat Vulnerability of Extreme Heat in Hangzhou via Comparing Two Approaches.	(X. Liu et al., 2020)	Demographic and socioeconomic data: Total population, population aged 65+, living alone, less education, unhealthy population over 60. Cooling facilities data: Public access to cooling facilities (e.g., supermarkets, shopping plazas and libraries) Green space data: Deciduous forest, evergreen forest, mixed forest, shrub, grassland, parks, and wetlands Health related death data: Cardiovascular diseases, respiratory diseases, heat stroke, dehydration, and hyperpyrexia were related to heatwaves. Vulnerability dimensions: i) Age and health status ii) Social isolation iii) Low-educated members iv) Economic factors v) Environmental exposure.
Mapping Heat Vulnerability Index Based on Different Urbanization Levels in Nebraska, USA.	(Jalalzadeh Fard et al., 2021)	i) Age over 60 ii) Age over 60 living alone iii) Below poverty line iv) Race other than white. v) English language barrier vi) Between 18 and 64 with disability, and vii) Education of less than high school diploma.
Socio-spatial Modeling for Climate-Based Emergencies: Extreme Heat Vulnerability Index.	(Stanforth et al., 2016)	i) Age 65 and older, female ii) Age 65 and older, male iii) Age 65 and older: female socially isolated iv) White race population v) Age 65 and older: male socially isolated vi) Mean family income.

		vii) Per capita income viii) Mean household income. ix) Adult population without high school diploma x) Asian race population xi) Age 65 and older. group living. xii) Hispanic race population xiii) Adult population with high school diploma xiv) NDBI xv) NDVI xvi) Black race population xvii) Land surface temperature.
Delineation of Spatial Variability in the Temperature–Mortality Relationship on Extremely Hot Days in Greater Vancouver, Canada	(Ho et al., 2017)	i) Average (range) deaths per day. ii) Percent male iii) Mean (SD) age at death (years) iv) Mean (SD) land surface temperature (°C) v) Mean (SD) air temperature (°C) vi) Mean (SD) humidex (°C) vii) Mean (SD) VANDIX viii) Mean (SD) percent not graduated from high school. ix) Mean (SD) unemployment rate (%) x) Mean (SD) percent with no university degree. xi) Mean (SD) percent of single parent families. xii) Mean (SD) average income ratio. xiii) Mean (SD) percent of homes rented. xiv) Mean (SD) labor nonparticipation rate. xv) Mean (SD) density of population ≥ 55 years (per km2) xvi) Mean (SD) density of persons living alone (per km2) xvii) Mean (SD) density of housing built before 1970.
2023 Heat Vulnerability Index Released by Multnomah County Health Department	(Office of Sustainability, 2023)	Exposure: i) People per Square Mile. ii) Housing Units per Square Mile. iii) Percent Tree Canopy Cover. iv) Percent Vegetative Cover. v) Percent Impervious Surfaces. vi) Annual Average Surface Temperature. Sensitivity: i) Population Under 18 Years of Age. ii) Population Over 65 Years of Age. iii) Population Over 65, Living Alone. iv) Male Population. v) Prevalence of Coronary Heart Disease. vi) Prevalence of Adults with Diabetes.

vii) Prevalence of Adults in Poor Physical Health.

Adaptive capacity:

i) Population with Less than a bachelor's degree.
ii) Population in Rental Housing.
iii) Population with Cognitive Difficulty.
iv) Foreign-Born Population.
v) Population Speaking English "Not Well".
vi) Black, Indigenous, and People of Color.

After an in-depth literature review and careful consideration, we selected vulnerability indicators (both exogenous and endogenous) and utilized a wide range of open data sources to complete this study. Utilization of open data has enabled rapid and convenient access to the required data and aided the completion of the study. Table 3.2 summarizes the data required for this study along with the appropriate sources where land surface temperature, no canopy cover and built-up area are Endogenous variables while the rest are Exogenous variables.

Table 3.2, Synopsis of the data sources for the variables employed in the analysis.

Index		Variable	Variable Description	Data & Year	Data Source
Exposure	1	Land Surface Temperature (LST)	Temperature of the Earth's Surface	Landsat 5 2006 2011	USGS
		Land Surface Temperature (LST)	Temperature of the Earth's Surface	Landsat 8 2016 2021	
	2	No Canopy Cover	Area Lacking Canopy Cover	Landcover 2005 2010 2015 2020	North American Environmental Atlas
	3	Built-up area	Built-up surfaces		
	4	Population density	Population density (per sq. km)	Census Data 2006 2011 2016 2021	Statistics Canada
Sensitivity	1	Male population	Proportion of male population in each DA	Census Data 2006 2011 2016 2021	Statistics Canada
	2	Very young population	Population per sq. km under 4 years old in each DA		
	3	Elderly population	Population per sq. km over 65 years old in each DA		

Adaptive Capacity	1	Low income HH	Proportion of households with low-income status	Census Data 2006 2011 2016 2021	Statistics Canada
	2	Living alone	Proportion of living alone population		
	3	Population with No knowledge of official language	Proportion of residents who are not acquainted with the official language		
	4	Private HHs rented	Proportion of private dwellings under rental contracts		
	5	Ethnicity	Proportion of ethnic /minor population		
	6	Population over 15 years old without high school degree	Proportion of 15 years and older population with no high school degree		
	7	Population over 15 years old with no fixed workplace	Proportion of 15 and above aged population without a permanent workplace		
	8	Population over 15 years old with no private car	Proportion of the 15 and above aged population without access to a private car		
	9	Non-Canadian population living in private HHs	Proportion of non-Canadian residents residing in private HHs		

Other Datasets

Serial No	Data	File Type	Year	Data Source
1	Dissemination Area	Shapefile (.shp)	2006 2011 2016 2021	Statistics Canada
2	Tax Designated Area	Shapefile (.shp)	N/A	
3	Country and Provincial Boundary	Shapefile (.shp)	N/A	
4	Population Center	Shapefile (.shp)	2011 2016 2021	
5	Regional Core	Shapefile (.shp)	N/A	HRM Open Data
6	Heritage Conservation Districts	Shapefile (.shp)	N/A	

3.3 Methods Overview:

Different combinations of exposure, sensitivity and adaptive capacity have been widely used by scholars to calculate HVI (Aminipouri et al., 2016; Conlon et al., 2020; Mallen et al., 2019; Sabrin et al., 2020). This study opted to identify the vulnerability indicators (summarized in table 3.2) and calculated the HVI for the urban area of HRM in 2006, 2011, 2016, and 2021 for this study. All the selected variables were prepared and

statistically analyzed before generating the model. Calculations were completed upon combining socio-economic data and remotely sensed satellite imagery. By adding exposure (E), sensitivity (S), and the adaptive capacity (A) scores, we then computed the HVI, which finally stands as:

$$HVI = E + S + A$$

In doing so, this study conducted five major steps, such as: (1) identification of data types and sources; (2) data acquisition and preprocessing; (3) Statistical analyses; (4) Calculations and Preparation of the HVI; and (5) Generating HVI to the dissemination area level. Figure 3.2 illustrates the diagram of methodological approach adopted in this study.

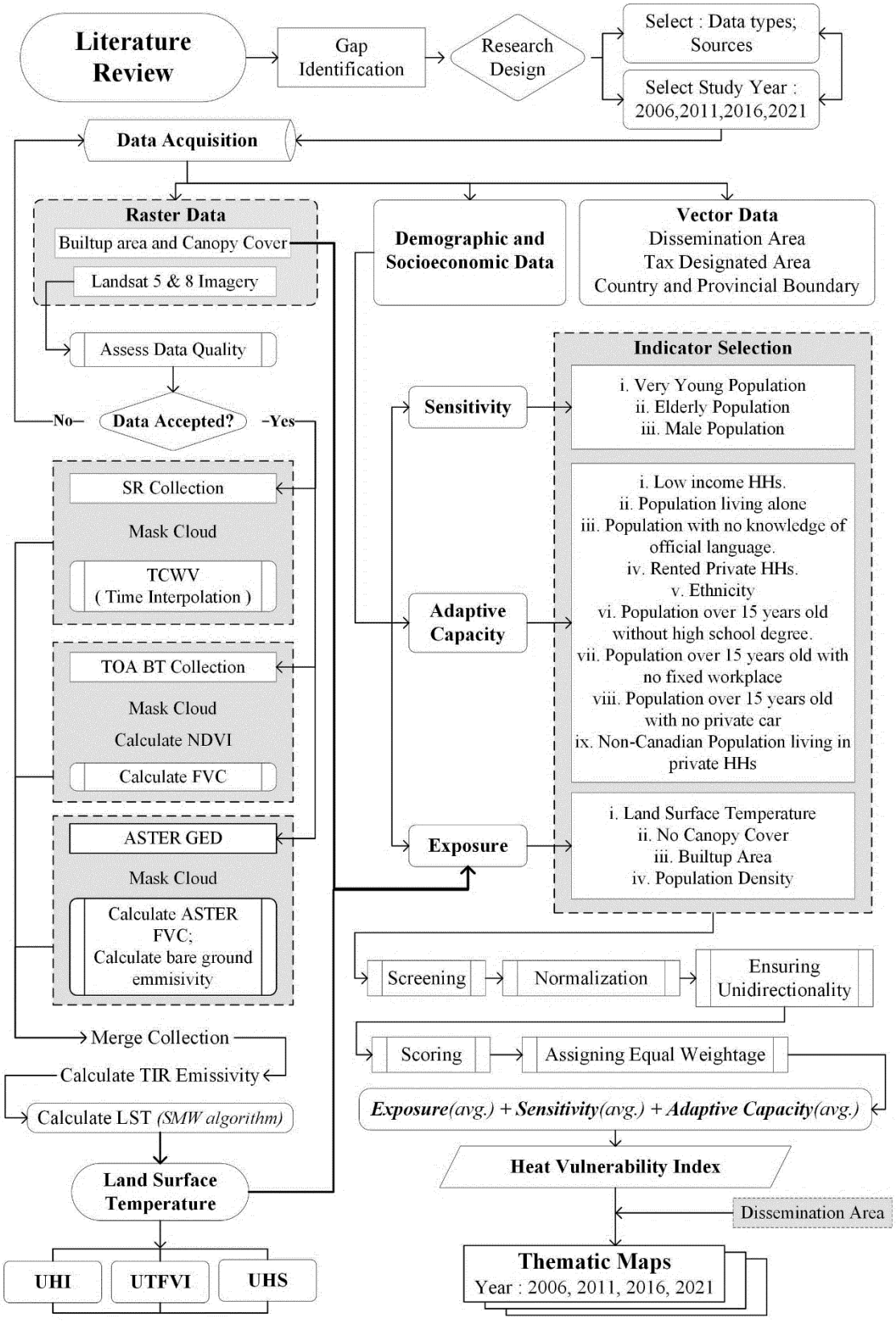

Figure 3.2, Schematic diagram of the adopted method of the study.

3.4 Identification of Data Types and Sources

Initially, this study identified a combination of different datasets and formats [i.e., Raster Data (e.g., Landsat 5 & 8 imageries; landcover data 2005, 2010, 2015, 2020); Census Data (e.g., population density, young population, population age over 65, minority status, education level etc.); Vector data (i.e., GIS Shapefiles)] in order to progress the study. Remote sensing data was captured from reliable sources (e.g., USGS, CEC North American Atlas and GEE) while vector data (e.g., dissemination area, tax designated area, and geographical boundaries etc.) were freely accessible from both Statistics Canada, and Halifax Open Data website.

3.5 Data Acquisition and Preprocessing

GIS datasets were mainly downloaded from Statistics Canada and Halifax Open Data website. Census data were obtained from Statistics Canada. The Canadian census is a valuable source of demographic and socio-economic data that provides insights into the country's population trends, characteristics, and distribution. One key aspect that varies between census years is the survey methodology and sample percentage. For instance, the 2006 and 2011 censuses were conducted using a mandatory long-form census questionnaire that was sent to a sample of households. However, in 2011, there was a shift to a voluntary National Household Survey (NHS) for the long-form questions, which led to concerns about data accuracy and representativeness due to a lower response rate.

In contrast, the 2016 and 2021 censuses reverted to a mandatory long-form questionnaire, ensuring a more comprehensive and reliable data collection process. This change allowed for a more detailed analysis of socio-economic characteristics such as income, education,

employment, housing conditions, and language spoken at home. Consequently, the raster data (e.g., Landsat 5 & 8 imageries) was acquired from USGS and Landcover datasets were extracted from the North American Environmental ATLAS website. This study utilized Landsat imagery from two satellites: Landsat 5 (1984-2013) and Landsat 8 (2013-present). Specifically, Landsat 5 imagery was chosen for the years 2006 and 2011, while Landsat 8 imagery was used for 2016 and 2021. Landsat 7 data was excluded due to known scan line errors, ensuring the highest quality data analysis. Afterwards, the preprocessing steps were conducted to make the data available for the model in an appropriate format. This procedure involved stages such as: reading meta files, checking and cleaning data, normalizing the information in an appropriate scale, ensuring unidirectionality of the information, filling the missing values, and converting the raw data into the required format, among various other technical steps.

3.5.1 Selection of Exposure Variables

Firstly, collections of Top of Atmosphere (TOA) brightness temperatures (BT), and Surface Reflectance (SR) for the study area were downloaded in GEE platform. Following that, a cloud mask was applied to both using the quality assessment bands. The SR data are, in turn, used to compute NDVI, which is then converted to FVC values using the subsequent formula.

$$FVC = \left(\frac{NDVI - NDVI_{bare}}{NDVI_{veg} - NDVI_{bare}}\right)^2 \quad (1)$$

Here, $NDVI_{bare}$ = NDVI estimates of completely bare pixels and $NDVI_{veg}$ = NDVI estimates of fully vegetated pixels. In accordance with earlier examinations (Jiménez-Muñoz et al., 2009; Prihodko & Goward, 1997; Ren et al., 2017; Tang et al., 2010; F.

Wang et al., 2015) , these two threshold values are set to $NDVI_{bare}$ = 0.2 and $NDVI_{veg}$ = 0.86. FVC values are then used together with previously computed ASTER emissivity values for bare ground to obtain the corresponding Landsat emissivity. The subsequent formula was employed for this purpose.

$$\varepsilon b = FVC_{\varepsilon b,\ \text{veg}} + (1 - FVC)\ _{\varepsilon b,\ \text{bare}} \quad (2)$$

Here, prescribed value of $\varepsilon b,\ veg$ = 0.99. $\varepsilon b,\ veg$ and $\varepsilon b,\ bare$ is the emissivity of vegetation and b = bare ground for a given spectral band. Finally, the SMW algorithm (3) is applied to the TOA TB of the Landsat TIR band.

$$\text{LST} = X_i \frac{Tb}{\varepsilon} + Y_i \frac{1}{\varepsilon} + Z_i \quad (3)$$

Here, T_b is the TOA brightness temperature in the TIR Channel, and Ɛ is the surface emissivity for the similar channel. The algorithm coefficients X_i, Y_i and Z_i are molded from linear regression of radiative transfer simulations performed for 10 classes of TCWV (I = 1,…,10) and are mapped onto the Landsat image The code and the look up table containing the coefficients are available to the users in the indicated repository shared by Ermida et al. (2020).

Table 3.3, Outlining the properties of the spectral bands sourced in this study for each Landsat satellite imagery.

Name of the Satellite	Bands Used	Wavelength (µm)	Dataset	Spatial Resolution	Image Dates
Landsat 5 (TM)	Red: B3 NIR: B4 TIR: B6	0.63–0.69 0.76–0.90 10.4–12.5	C01/T1_SR C01/T1_SR C01/T1_TOA	30 m 30 m 120^2 m	3 July 2006 and 21 August 2011
Landsat 8 (OLI; TIRS)	Red: B4 NIR: B5 TIR: B10	0.64–0.67 0.85–0.88 10.6–11.19	C01/T1_SR C01/T1_SR C01/T1_TOA	30 m 30 m 100^2 m	21 August 2016 and 16 August 2021

Also, the built-up area and the canopy covered area were extracted from the Land Cover Data provided by North American Environmental Atlas. As the canopy cover was considered as an exposure variable, to ensure unidirectionality of the data it was subtracted from 100 to get the area lacking canopy cover or simply to get the extent of exposed ground. So, the final variable was calculated as:

$$No\ Canopy\ Cover = 100 - (Canopy\ Cover)$$

Zonal statistics for each dissemination area (2006,2011,2016,2021) were calculated (averaged) using ArcGIS Pro 3.2.1.

3.5.2 Sensitivity Variables

To qualify for sensitivity, this study chooses three variables from the census database, as specified in table 3.2: 1) male population, 2) very young population and 3) elderly population. Children included those four years or younger. For elderly population variable proportion of 65 years of age or older individuals were included.

3.5.3 Adaptive Capacity Variables

Quantifying adaptive capacity employed nine variables (Table 3.2) : 1) low-income households variable includes proportion of households with low-income status after tax, 2) Living alone variable includes proportion of living alone population in private households, 3) Population with no knowledge of official language variable includes the proportion of residents who are not acquainted with the official language(English/French), 4) Private HHs rented variable includes the proportion of private dwellings under rental contracts, 5) Minor population variable includes the proportion of minority population in the community, 6) Population over 15 years old without high

school degree variable includes the proportion of 15 years and older population with no high school degree, 7) Population over 15 years old with no fixed workplace variable includes the proportion of 15 and above aged population without a permanent workplace, 8) Population over 15 years old with no private car variable includes the proportion of the 15 and above aged population without access to a private car, and 9) Non-Canadian population living in private HHs variable includes the proportion of non-Canadian residents residing in private households.

3.6 Statistical analysis

Statistical analyses were performed using MS Excel and then incorporated into the spatial datasets. This study excluded all the census dissemination areas where the population is zero. Beforehand, this study normalized all the variables by dividing the numerator (intervention population) by denominator (total eligible population). The following scoring mechanism was applied to each component:

$$\text{Z-Score} = \frac{[Observed\ value - Mean_x]}{Std.\ deviation}$$

To accomplish the final Z-score this study adopted the scoring scheme from Reid et al., 2009. It is presented on table 3.4 (Reid et al., 2009). An example of the Z-score is included in the appendix section.

Table 3.4, HVI scores assigned to each component in this study.

Range of Z-Score	Assigned HVI Component Score
-2 or lower	1
-2 to -1	2
-1 to 0	3
0 to 1	4
1 to 2	5
2 or higher	6

3.7 Calculations and Preparation of the HVI

Employing a succession of "nested if statements", the ultimate score was obtained and subsequently this process was iterated for each indicator. The EWA was employed for the weighting of all indicators in the construction of the HVI_{EWA}. The ultimate representation of the HVI_{EWA} is outlined below:

$$HVI_{EWA} = \overline{E} + \overline{S} + \overline{A}$$

Here, $\overline{E}$ = Average of all Exposure Variable, $\overline{S}$ = Average of all Sensitivity Variables, $\overline{A}$ = Average of all Adaptive Capacity Variable

3.8 Mapping HVI to the Dissemination Area Level:

In this stage, weighted HVI_{EWA} scores were added to the dissemination area shapefiles (2006, 2011, 2016, 2021) in ArcGIS Pro and HVI_{EWA} maps were produced to demonstrate the findings for different periods. These maps were prepared at dissemination areas (DA), to demonstrate local units of a census district.

3.9 Estimating UHI index, UTFVI and UHS:

3.9.1 Urban Heat Island (UHI) Index:

Heat islands are urbanized areas that experience higher temperatures than outlying areas. The heat island effect can result in significant temperature differences between rural and urban areas(EPA - U.S. Environmental Protection Agency, 2012; Yang et al., 2016). This study classified LST maps into five temperature classes using means and standard deviation to create a UHI index (Amindin et al., 2021; Xu et al., 2013) (Table 3.5).

Table 3.5, UHI scores assigned to each component in this study.

Class range	Class name
$T \leq T_{Mean} - 1.5std$	Very cold temperature
$T_{Mean} - 1.5std < T \leq T_{Mean} + std$	Cold temperature
$T_{Mean} + std < T \leq T_{Mean} - std$	Moderate temperature
$T_{Mean} - std < T \leq T_{Mean} + 1.5std$	Hot temperature
$T > T_{Mean} + 1.5std$	Very hot temperature

3.9.2 Urban Thermal Field Variance Index (UTFVI):

UTFVI serves as a commonly employed index for a more precise characterization of the Surface Urban Heat Island (SUHI) effect (Naim & Kafy, 2021; Tomlinson et al., 2011a). Areas exhibiting a significantly higher temperature than the adjacent rural areas correspond to elevated concentrations of UTFVI (Naim & Kafy, 2021; H. Wang et al., 2017). The consequential impacts of UTFVI are extensive, encompassing adverse effects on local wind patterns, humidity levels, air quality, decreased comfort, increased mortality rates, and indirect economic losses, among other factors (Sejati et al., 2019). This study utilized UTFVI to systematically quantify the impact of the UHI and is calculated using the subsequent formula. (Amindin et al., 2021; L. Liu & Zhang, 2011; Zhang et al., 2006):

$$UTFVI = \frac{\Delta T}{T_S} = \frac{T_S - T_M}{T_S}$$

Where, T_S is the land surface temperature (LST), and T_M is the average temperature of the entire study area. To prepare an UTFVI map, each of the six classes created for the UTFVI classification map was assigned excellent, good, normal, bad, worse, and worst according to the values (Table 3.6) (Amindin et al., 2021; Renard et al., 2019; Zhang et al., 2006).

Table 3.6, UTFVI scores assigned to each component in this study.

UFTVI	Urban heat island phenomenon	Ecological evolution index
<0.00	None	Best
0.00–0.005	Very cold temperature	Better
0.005–0.010	Cold temperature	Normal
0.010–0.015	Moderate temperature	Bad
0.015–0.020	Hot temperature	Worse
>0.020	Very hot temperature	Worst

3.9.3 Urban Heat Hotspot Mapping:

A localized region exhibiting notably elevated temperatures within an urban setting is termed an urban heat hotspot. To enhance comprehension of the UHI effect, mapping of these urban heat hotspots was conducted. The identification of UHS (Urban Heat spots) and Non-UHS areas involved the application of the following mechanism (Guha et al., 2017):

$$UHS = LST > \mu + 2\alpha$$

$$Non - UHS = LST < \mu + 2\alpha$$

Here, μ and α are the mean and standard deviation of LST in the study area, respectively.

Chapter 4: Result

4.1 Exposure:

In generating the heat exposure map of the study area, LST maps were created (Fig.4.1). After this, the heat exposure map is summarized in Fig 4.2.

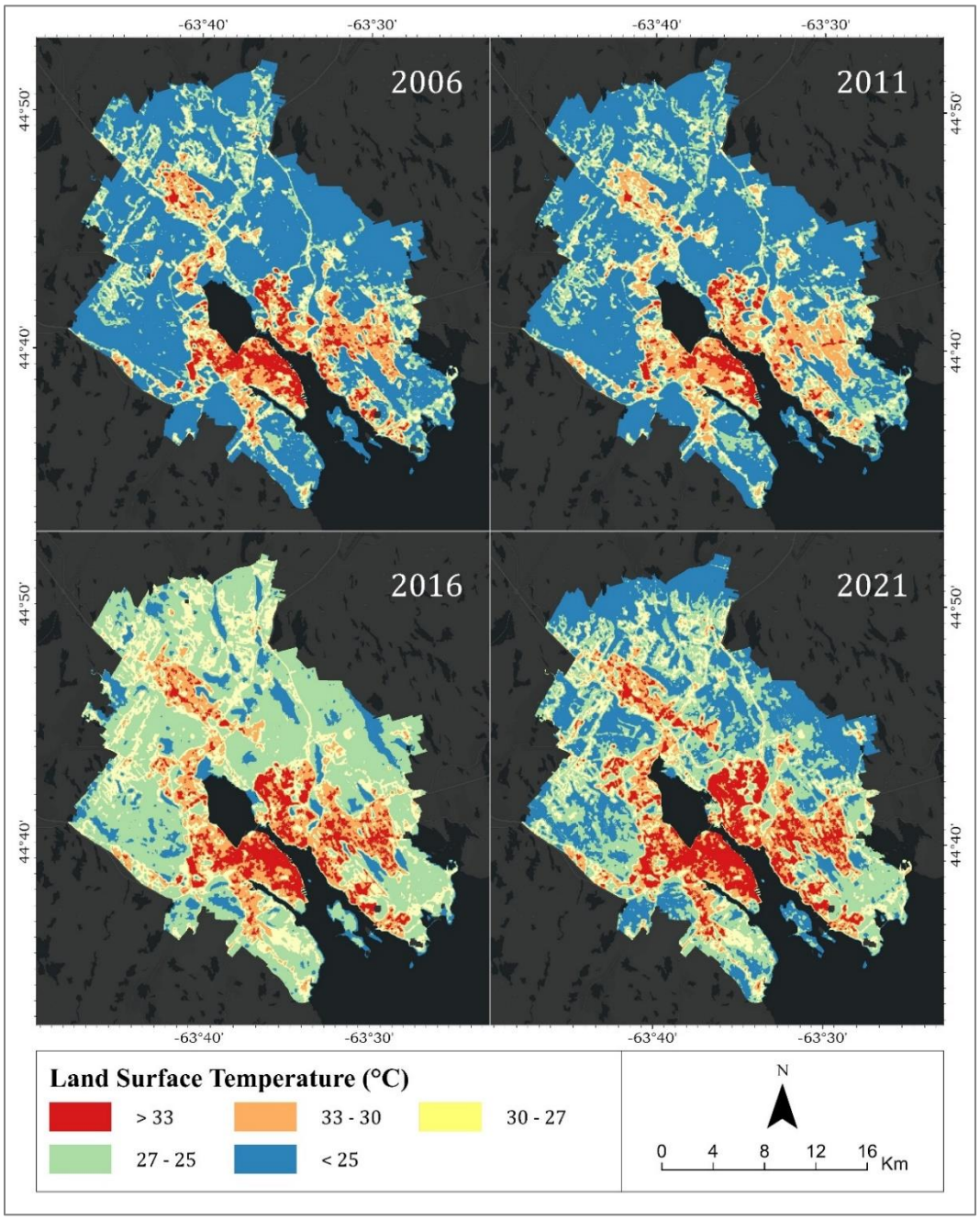

Figure 4.1, Summarizes the weighted exposure of land surface temperature in the study area.

Land Surface Temperature (LST) distribution followed a non-uniform pattern over the years considered, with LST of 2016 (August) and 2021 (August) are relatively higher on the same day in comparison with 2006 and 2011. Highly developed built-up areas on the Halifax peninsula and Dartmouth area show higher daily average LST while comparing with the suburbs (e.g., Bedford, Sackville, etc. areas). It is worthwhile to mention that the images depict only the average surface temperature of the ground on specific days (see table 3.3 3 for details) during the summer months (i.e., July and August only). Additionally, the ground surface captured in these images comprises various types, such as vegetation, water bodies, urban areas, etc., each with its own thermal properties. Therefore, the depicted temperature values are influenced by this mix of surface types within each pixel, contributing to variations in temperature across the image.

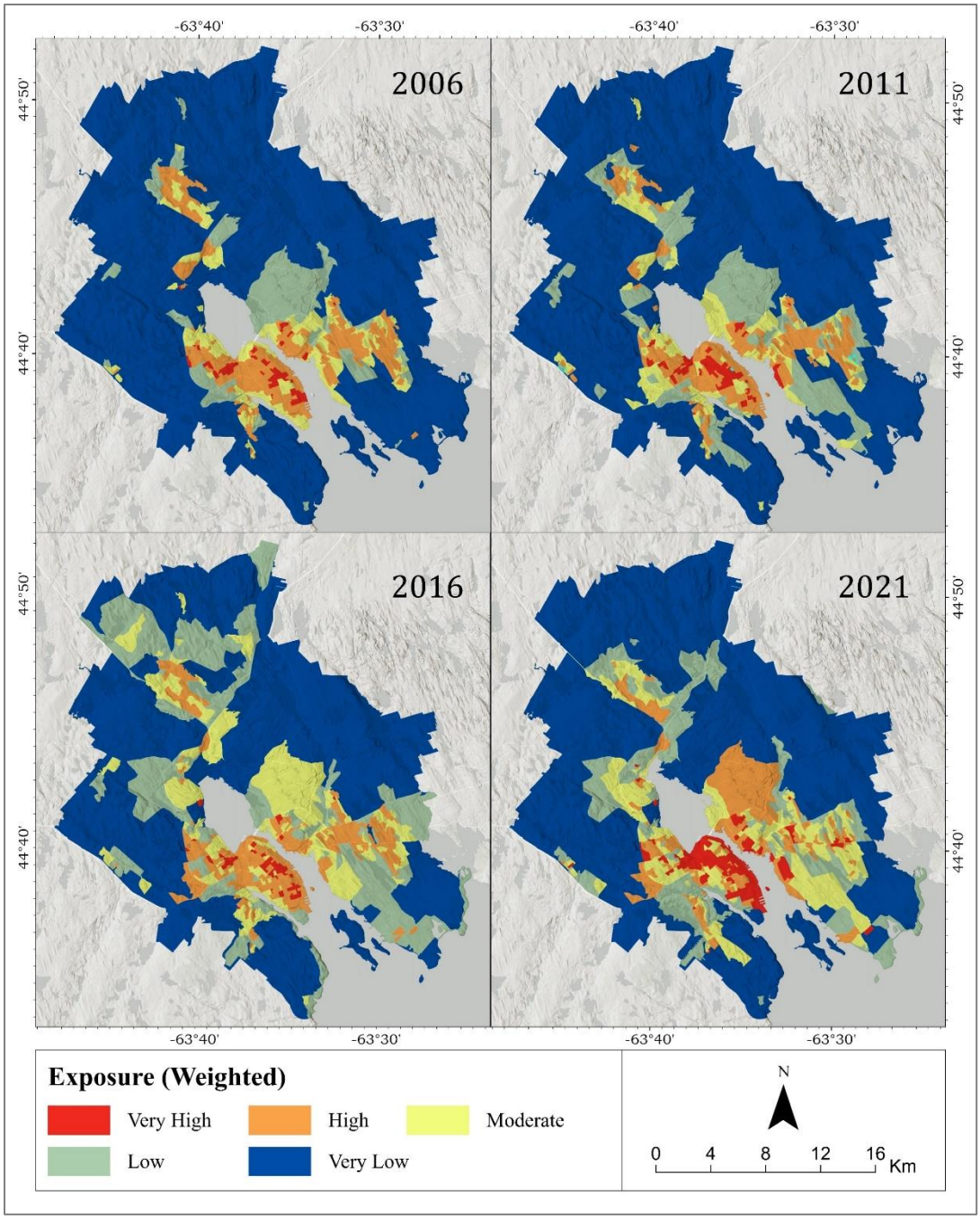

Figure 4.2, Weighted heat exposure index calculated for the study area.

Figure 4.2 shows the average weighted value of heat exposure in the study area upon considering values of LST, built-up area, canopy coverage and population density per square kilometer as exposure variables. The highest exposure values are found in the

peninsula across all the considered years. Heat exposure values have been consistently intensifying throughout the study area from 2006 until 2021. Note that the regional center has been experiencing an influx of population density that may have contributed to a growing surface temperature. The highest value of exposure is observed in the urban core that indicates a higher presence of impervious surfaces and buildings, coupled with reduced green vegetation and open spaces (e.g., bare soil, construction area, road surface, etc.). In contrast, the exposure values decrease when someone move away from the city center area. Areas like Cow Bay, Herring Cove, Hammonds Plains, and Timberlea on the outskirts of the city exhibit lower exposure values attributed to the cooling effects of abundant open parks and green spaces. The average exposure scores span between 7 to 11, where 7 means the lowest, 9-10 means moderate, and 11 indicates the highest probable exposure.

4.2 Mapping the Heat Sensitivity

The key variables for heat sensitivity analysis in this study are the male population, very young population, and elderly population. The findings indicate a that 2006 had the largest area of high sensitivity, measuring 237.77 sq. km, in the year 2006. This observation may be attributed to the presence of both very young (under 4 years) and elderly (over 65 years) populations situated in the suburban or rural areas and outside the regional core of the city. Population growth since then may have added more middle-aged and young people, thereby reducing the sensitivity as these groups are better able to handle excessive heat.

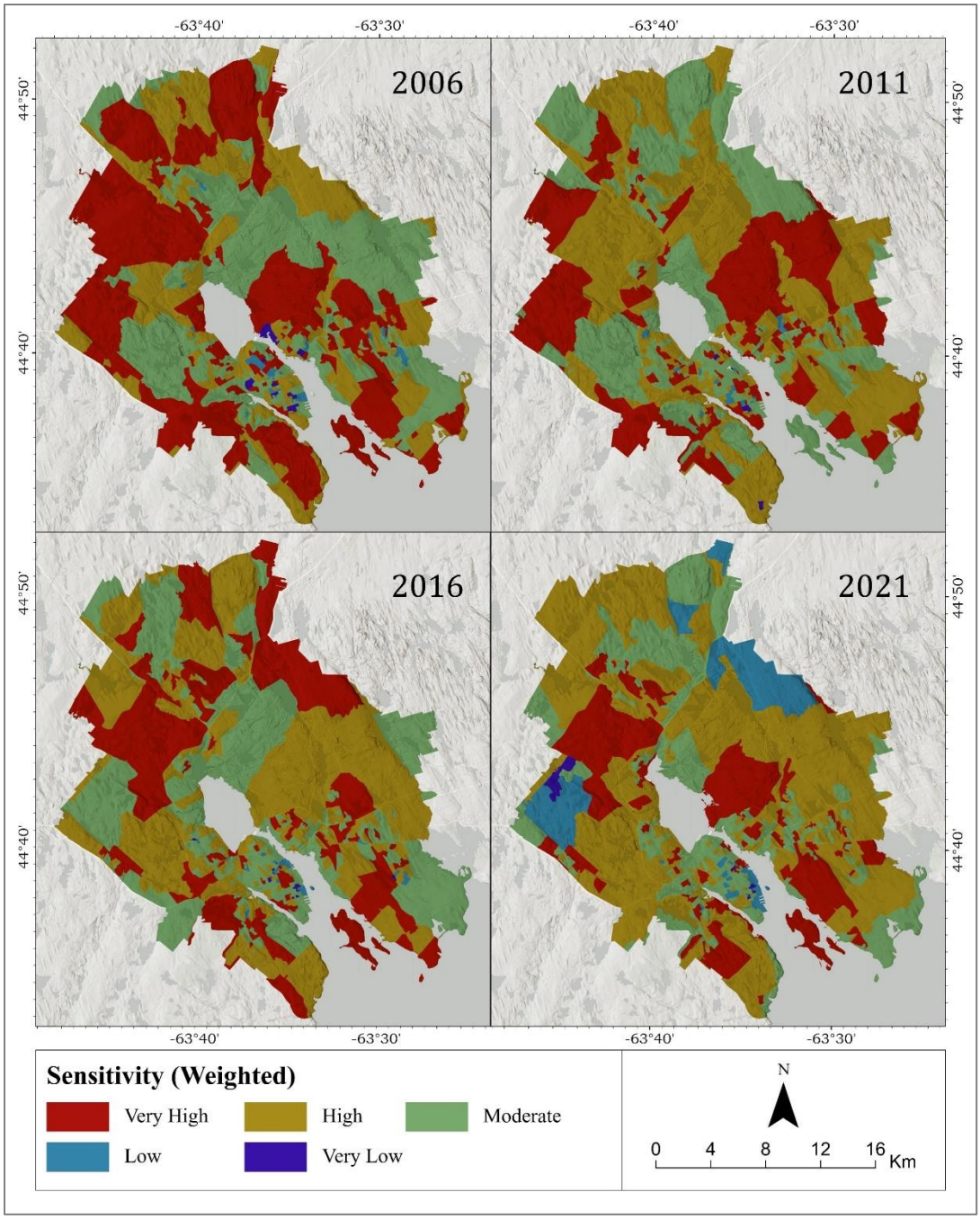

Figure 4.3, Summarizes the weighted heat sensitivity map of the study area.

Figure 4.3 reveals that there is a discernible increase in high sensitivity values (ranging from 3.39 to 3.86) in 2016 (233.58 sq. km) and 2021 (286.22 sq. km), compared to the 2006 scenario where the high-sensitivity area has been pointed 141.49 sq. km (refer to

table 4.1 for details). This suggests a constant increase in the numbers of elderly populations over time across the study area that contributes to upsurge the sensitivity index values. Notably, for the year 2011, 2016, and 2021 the sensitivity index value in the study area changed from very high (>3.86) to high (3.39-3.86) in comparison to other classes. It is worth highlighting that sensitivity does not exhibit a clear trend of change over the years (see table 4.1 for details), emphasizing the complexity and variability of demographic dynamics in the study area.

4.3 Mapping the Adaptive Capacity of the Study Area:

Based on previous literature outlined above, individuals with higher income, those living with their families, owning houses and cars, having higher education, having a fixed workplace and being Canadian citizens exhibit greater adaptability. The average adaptive capacity scores span between ≤ 2.6 to > 4.4, where 2.6 means the greatest capacity for managing heat stress, 3.2 – 3.8 exemplifies moderate, and > 4.4 indicates the lowest probable adaptability. In 2006, the regional core emerges as having less adaptive capacity than other places within the study area. The majority (52.02%) fell within the 2.60 – 3.20 range, which depicts a high value of adaptive capacity in other surrounding areas. A similar pattern persists in 2011, with a majority of areas in the outer region (suburban area) displaying moderate and high adaptive capacity. However, adaptive capacity increases in the subsequent years, where both 2016 and 2021 show average values of adaptive capacity across most of the areas. Additionally, suburbs (i.e. North Preston) stands out with the lowest value of adaptive capacity, suggesting that people in this area possess a lower income, highest rate of tenancy status, and have a lower level of education. In summary, the study indicates a positive trend of adaptive capacity in the

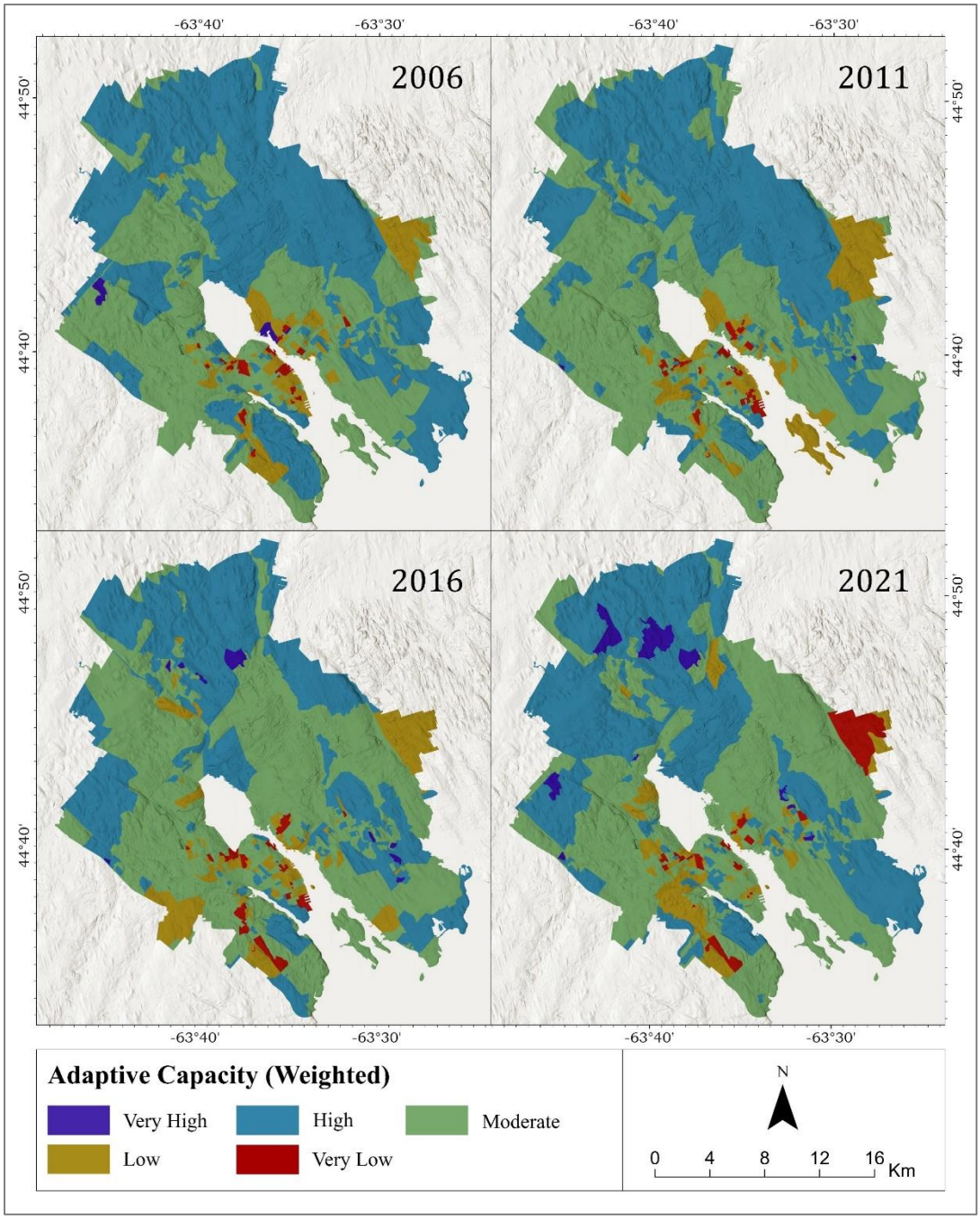

Figure 4.4, Summarizes the weighted Adaptive Capacity in the study area.

study area over the past decade. In 2006, the proportion of areas demonstrating very high adaptability stood at 0.38%, and by 2021, this figure had surged to 11.51%. A similar pattern was noted for regions characterized by very low adaptability, with specific details

available in Table 3.5. The key factors contributing to adaptability include higher income, family living, homeownership, car ownership, higher education, stable workplaces, and Canadian citizenship.

4.4 Mapping the Heat Vulnerability Index (HVI) for the Study Area

The HVI combines exposure, sensitivity, and adaptive capacity. The study establishes a positive relationship between exposure and HVI. The majority of areas characterized by Very High and High Index values for Exposure and HVI are found within the regional center. The HVI categorizes areas divided into five classes: very low (≤7.14), low (8-9), moderate (9-10), high (10-11), and very high (>11). In 2006, the peninsula and Dartmouth area exhibited the highest HVI values, surpassing 11. Concentrations of high and very high HVI values are predominantly observed in the population center (i.e. Dartmouth, Herring Cove, and Lower Sackville) ranging between 10 to 11. Areas with very low HVI index values are characterized by values of 7.14 or lower. By 2011, the percentage of moderate values increases, especially in the peninsula and its surrounding areas (Burnside, Cole Harbor, Hammonds Plain), where the values range between 9 and 11. In 2016, the study area exhibited predominantly moderate to high HVI values, suggesting heightened exposure and sensitivity concomitant with diminished adaptive capacity. Subsequently, upon scrutinizing the suburban areas (i.e. North Preston and Spryfield), a consistent erosion in adaptive capacity from low to very low levels was observed. Consequently, by 2021, some of the suburban areas (i.e. North Preston and Spryfield) underwent a transition from a state of moderate heat vulnerability to one characterized as highly heat vulnerable.

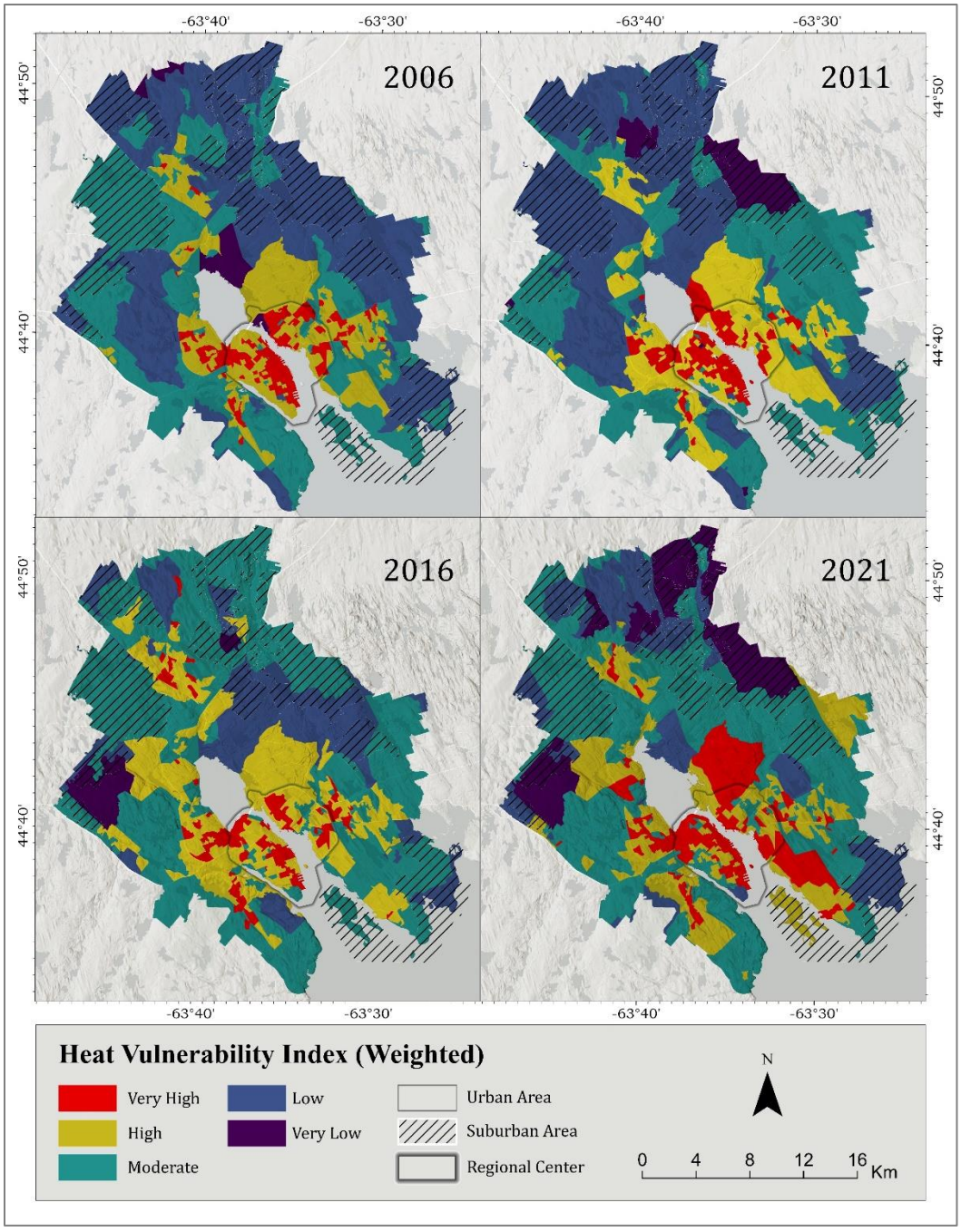

Figure 4.5, Summarizes the weighted HVI of exposure, adaptive capacity, and sensitivity in the study area.

In 2021, a distinct pattern emerges while explaining the HVI index. The highest HVI values are concentrated in the urban core areas (i.e. peninsula Halifax, Clayton Park Area, Dartmouth, Herring Cove, Eastern Passage) and sporadically distributed in and around

Lower Sackville and Lakeview. Because of moderate to very low adaptive capacity in the regional center of Halifax these areas exhibit very high HVI index values (area 58.41 sq. km). Elevated exposure and sensitivity stemming from high population density, increased land surface temperature, and limited canopy coverages is observed. Very low HVI values mainly exist in the north-east part of the study area. This is because both sensitivity and exposure index values are comparatively lower in this part of the study area. They also received a low score for adaptive capacity variables. Although this study didn't consider building/infrastructure age/condition during the calculation of HVI, upon examination it was observed that 90% of the heritage conservation district fell within the high and very high HVI classes.

4.5 Summarizing the Analyzed Information:

Here the percentages of areas exposed to HVI and other considered indicators were summarized. Note that approximately 45% of areas (i.e., 254.99 sq. km) demonstrate moderate values of HVI. Interestingly, very high HVI (10.39%) and very low HVI (11.42%) areas are almost similar. However, concentration of high HVI areas is found in and around the downtown of both Halifax and Dartmouth region (Fig 4.3 for details).

Table 4.1, Provides a summary of the total area, delineated by class, measured in square kilometers, for each study year and across all 3 variables (Exposure, Sensitivity, Adaptive Capacity) and HVI.

	Variables	**2006**		**2011**		**2016**		**2021**	
		Area		**Area**		**Area**		**Area**	
	Exposure	Sq. Km	%	Sq. Km	%	Sq. Km	%	Sq. Km	%
Class	Very High	4.89	0.86	6.93	1.23	4.19	0.74	16.82	2.99
	High	45.56	8.07	42.94	7.61	46.35	8.21	47.18	8.39
	Moderate	31.43	5.57	35.96	6.37	68.79	12.18	58.29	10.37
	Low	45.89	8.13	67.04	11.87	118.18	20.93	75.37	13.40
	Very Low	436.72	77.36	411.69	72.92	327.05	57.93	364.61	64.85
	Sensitivity								
Class	Very High	237.77	42.12	154.9	27.44	156.3	27.68	106.4	18.92
	High	141.49	25.06	233.58	41.38	223.85	39.65	286.22	50.90
	Moderate	179.03	31.72	173.23	30.68	181.81	32.20	120.21	21.38
	Low	3.79	0.67	2.14	0.37	2.09	0.37	46.75	8.31
	Very Low	2.41	0.43	0.65	0.11	0.51	0.09	2.69	0.48
Adaptive Capacity									
Class	Very High	2.16	0.38	0.26	0.05	3.24	0.57	11.51	2.05
	High	293.67	52.02	240.43	42.59	208.44	36.92	239.37	42.57
	Moderate	219.53	38.88	271.45	48.08	301.82	53.46	264.82	47.09
	Low	43.55	7.71	47.57	8.43	44.46	7.87	31.83	5.66
	Very Low	5.59	0.99	4.79	0.85	6.59	1.17	14.75	2.62
	HVI								
Class	Very High	26.16	4.63	28.48	5.04	24.1	4.27	58.41	10.39
	High	83.77	14.84	95.42	16.90	124.02	21.97	96.27	17.12
	Moderate	224.05	39.69	188.7	33.42	298.37	52.857	254.99	45.35
	Low	218.31	38.67	231.96	41.09	101.36	17.96	88.41	15.72
	Very Low	12.19	2.16	19.96	3.53	16.71	2.96	64.19	11.42

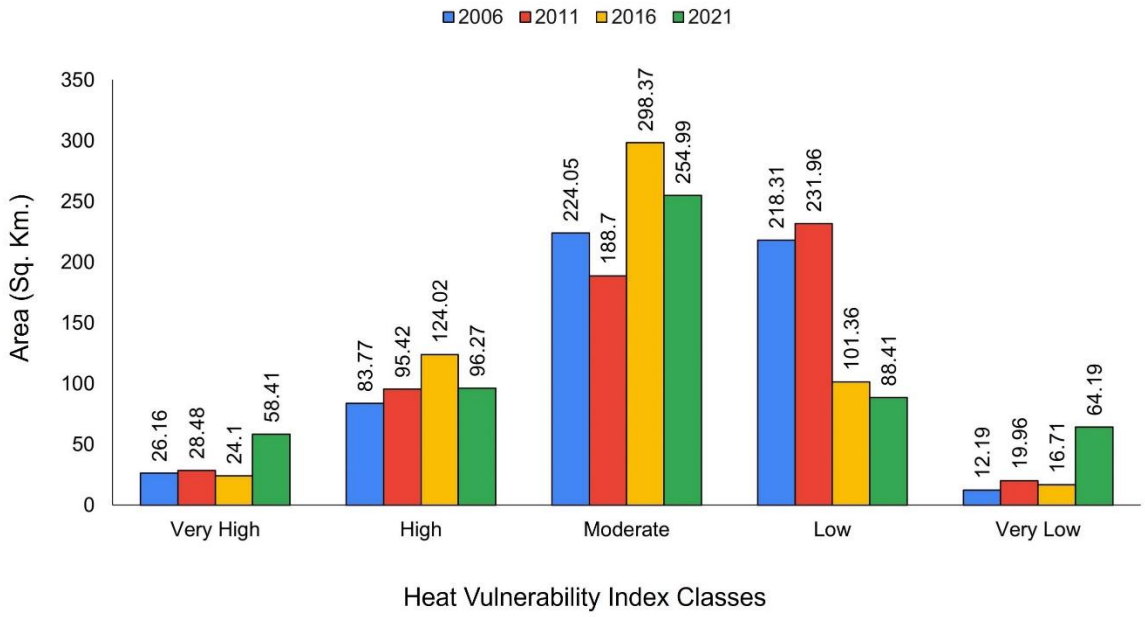

Figure 4.6, Exhibits the changes of overall HVI area (Sq. Km), categorized by class, across each year considered in the study.

Conversely, North Preston and the outer regions of HRM and Dartmouth showcase very low adaptive capacity and are indexed as high HVI. This is attributed to a high number of low-education and low-income individuals in these areas. Figure 4.4 illustrates a notable increase in both very high (58.41 sq. km) and very low (64.19 sq. km) heat-vulnerable areas in 2021 when contrasted with the corresponding values for the remaining three years. According to Figure 6, a majority of the areas in the study area are demonstrating moderate HVI values for 2006, 2011 and 2016. However, 2021 shows the highest percentage of HVI value while comparing with other years. This certainly demonstrates the potential impacts of climate change, population increase, and more vulnerable people living in the communities. Interestingly, very low heat vulnerable areas have increased in 2021. This may be one of the reasons for having more young population in the society along with opportunities to more jobs in the regional center.

Table 4.2, Provides a breakdown of the total number of people in each HVI class, along with their corresponding percentages.

HVI		2006		2011		2016		2021	
		Total Population	%	Total Population	%	Total Population	%	Total Population	%
Class	Very High	86342	26.97	91909	27.41	77475	22.22	119595	31.25
	High	123189	38.49	126052	37.59	154984	44.46	125156	32.70
	Moderate	75054	23.45	76145	22.71	99234	28.46	105360	27.53
	Low	34394	10.75	37469	11.17	14931	4.28	23169	6.05
	Very Low	1106	0.35	3782	1.13	2006	0.58	9454	2.47

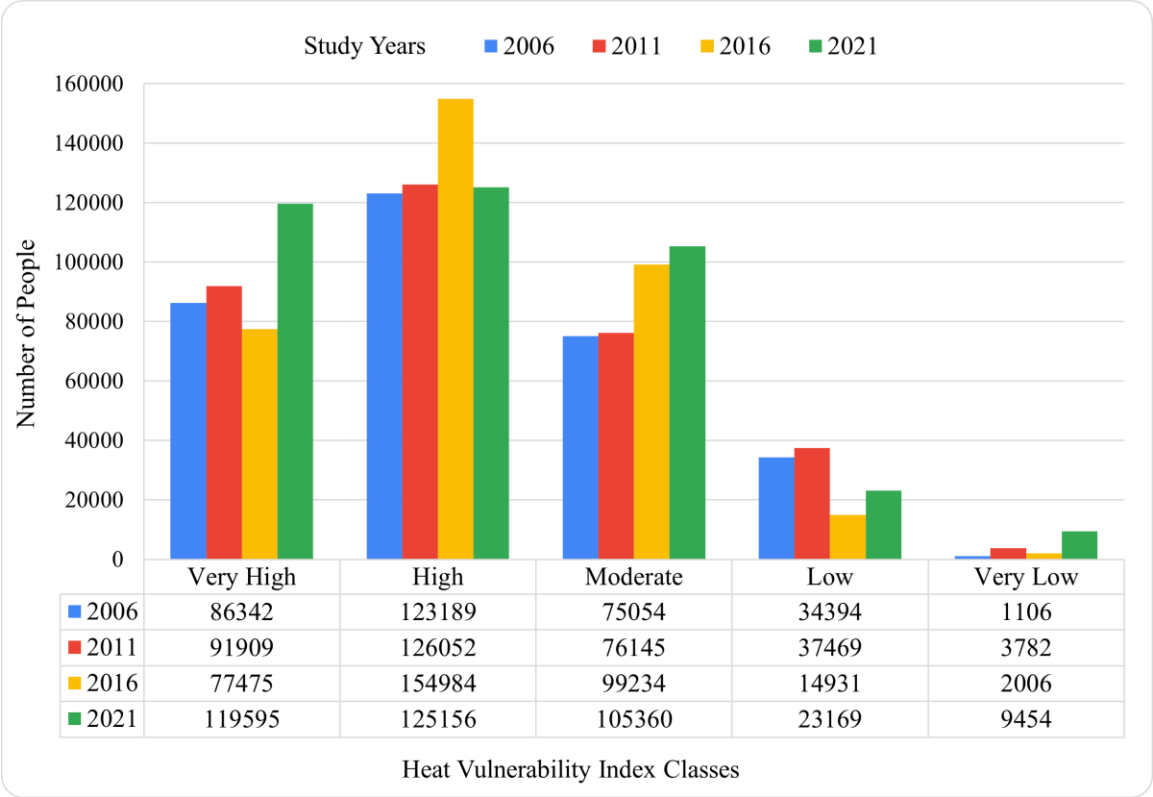

Figure 4.7, Exhibits total number of people in the HVI, categorized by class, across each year considered in the study.

The number of people in the 'Very High' HVI class has increased over the four study years with more people in the 'Very High' class than in any other class across all four years (Figure 4.7). In all four years, the most common HVI class is High. The number of

people in the Very High index class has increased over time. The number of people in the Low and Very Low HIV index classes have decreased over time.

4.6 Mapping Urban Heat Hotspots in the study area

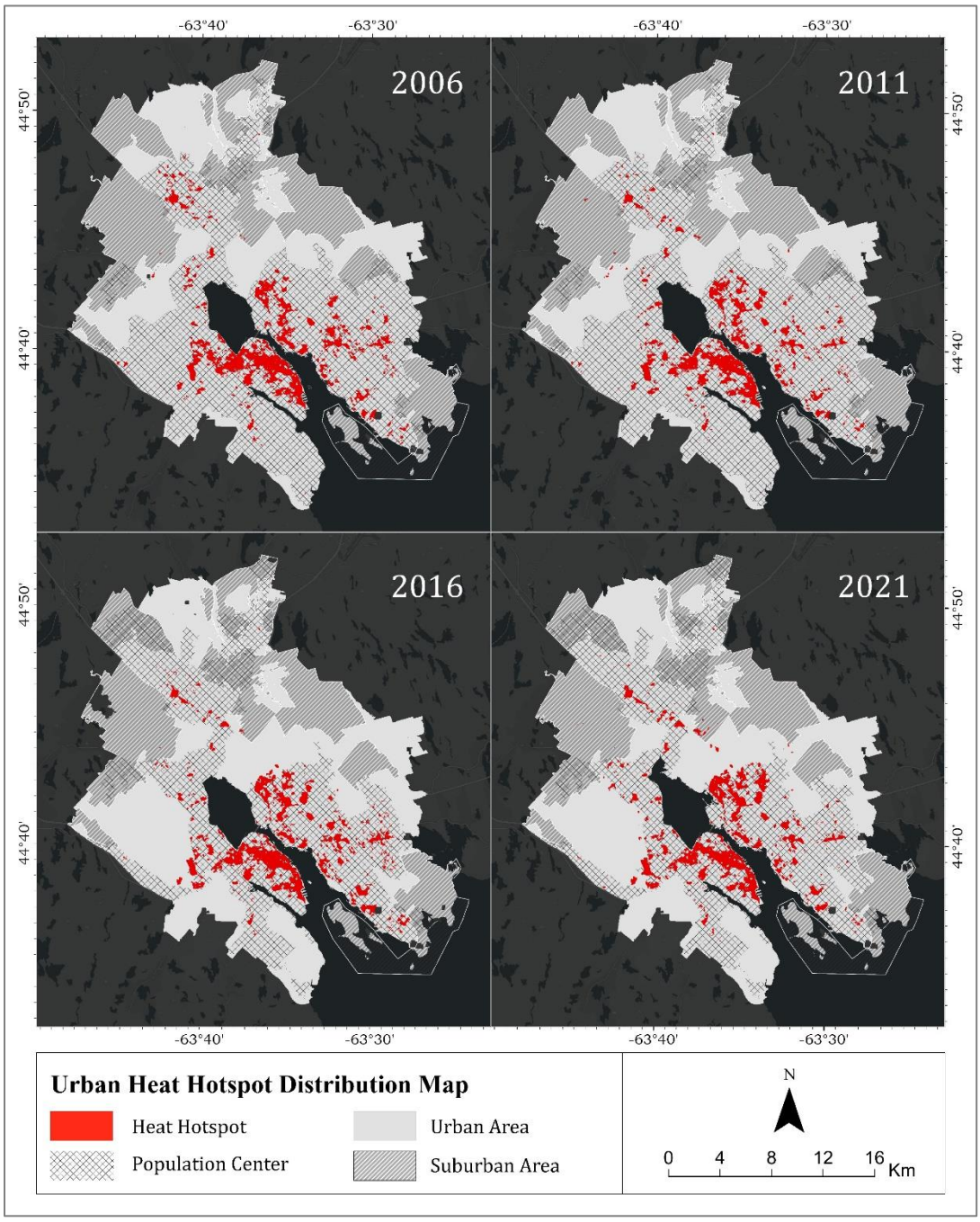

Figure 4.8, Exhibits the distribution of Urban Heat Hotspot in the study area.

Heat hotspots areas are mostly within population centers for all study years. Hotspots are dense in the regional core areas, specifically in the peninsula it is highest. Hotspots are quite scarce in suburban and outlying regions away from population centers.

4.7 Mapping Urban Heat Island in the Study Area

Figure 4.8 exhibits UHI map for the study area where red color represents very hot temperature areas and deep blue color represents very cold temperature areas.

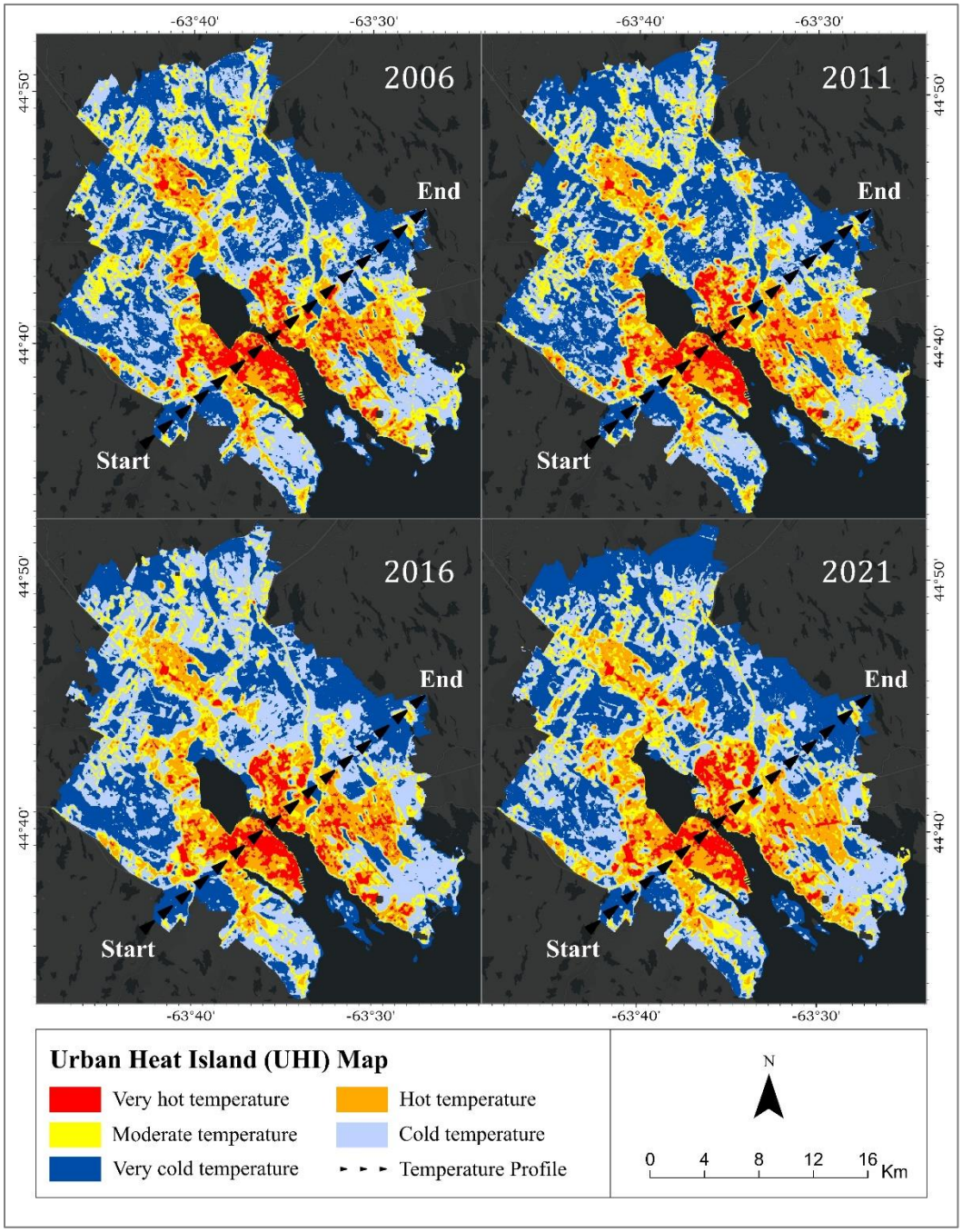

Figure 4.9, exhibiting spatial distribution of Urban Heat Island in the study area.

Please consult table 4.2 for a breakdown of UHI categories and their respective area percentages in Halifax for the years 2006, 2011, 2016, and 2021.

Table 4.3, Showing classification of urban heat island index (UHI) and their percentage of area in Halifax during 2006, 2011, 2016 and 2021.

Year	UHI categories with corresponding percentage of area (%)				
	Very cold temperature	Cold temperature	Moderate temperature	Hot temperature	Very hot temperature
2006	31.64	33.67	16.53	12.17	5.99
2011	34.99	29.75	16.02	13.93	5.31
2016	30.88	35.42	14.39	13.63	5.68
2021	34.71	30.93	14.3	14.71	5.34

Furthermore, to quantitatively analyze the UHI effect, the Urban Thermal Field Variance Index (UTFVI) was calculated (figure 4.9) for all study year. This index was derived from LST, and it determines the severity of UHI. It can be used to quantitatively analyze the UHI effect and be divided into six levels (best, better, normal, bad, worse, worst) in line with six specific ecological evaluation indices (table 3.6, 4.3 and figure 4.9).

Table 4.4, Showing classification of ecological evolution index UTFVI and their percentage of area in Halifax during 2006, 2011, 2016 and 2021.

Year	UTFVI categories with corresponding percentage of area (%)					
	Best <0.00	Better 0.00–0.005	Normal 0.005–0.010	Bad 0.010–0.015	Worse 0.015–0.020	Worst >0.020
2006	63.39	1.25	0.95	0.93	0.84	32.65
2011	62.44	1.66	1.01	1.03	1.04	32.82
2016	64.17	1.72	1.33	1.23	1.17	30.38
2021	63.74	1.25	0.95	0.91	0.86	32.28

4.8 Mapping Urban Thermal Field Variance Index (UTFVI) in the Study Area

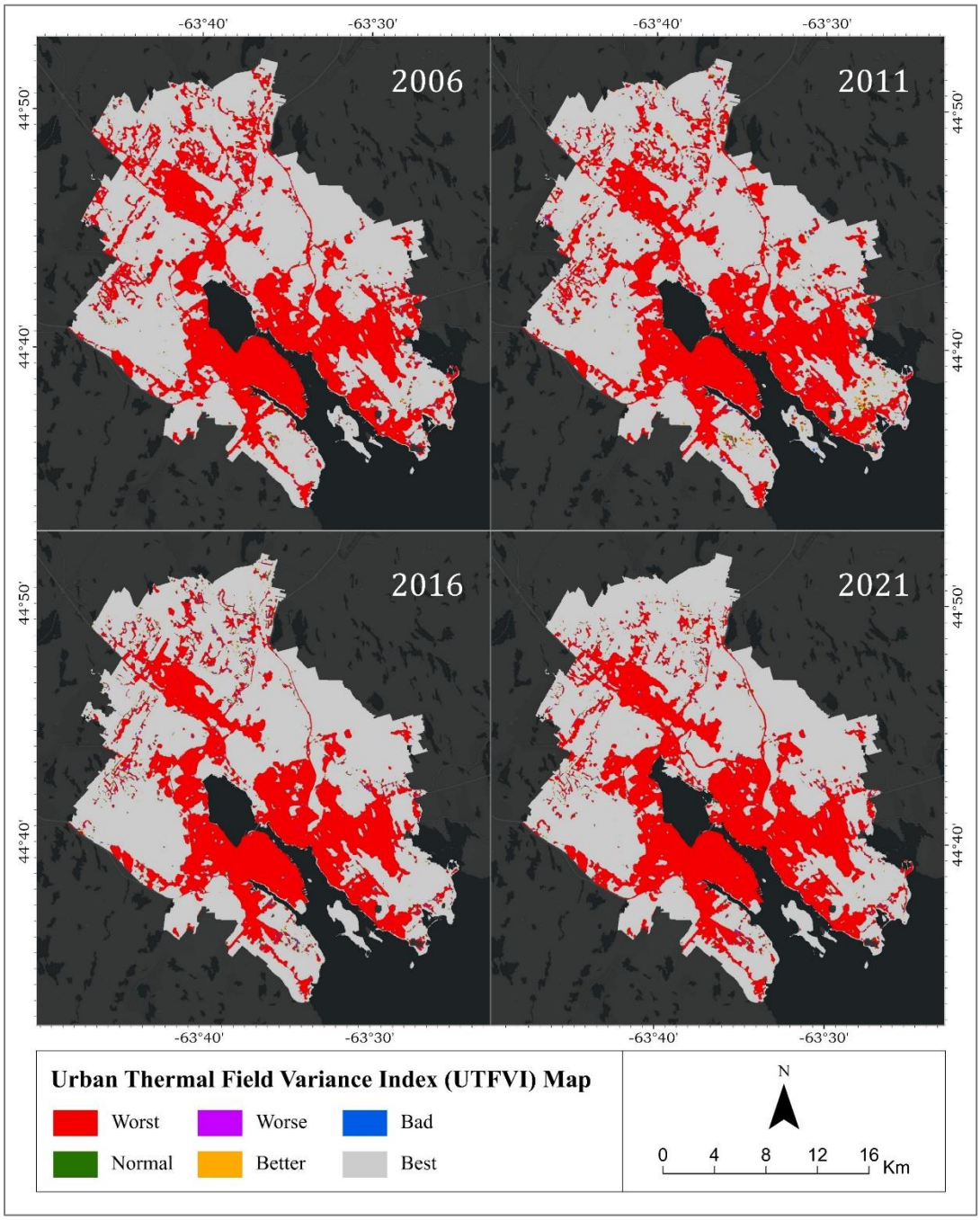

Figure 4.10, demonstrating Urban Thermal Field Variance Index (UTFVI) Map

Chapter 5: Discussion

Existing studies (Brooks et al., 2005; Cardona et al., 2012; Downing et al., 2005; Gaillard, 2010; Rathi et al., 2022) delineates the association between adaptive capacity and vulnerability through three distinct lenses. Firstly, previous research underscores the non-mutually exclusive nature of vulnerability and adaptive capacity. Secondly, vulnerability is posited as an outcome stemming from deficient adaptive capacity, alongside various other contributing factors. Thirdly, a reciprocal inverse relationship characterizes both, implying that heightened adaptive capacity corresponds to diminished vulnerability, and vice versa. In the context of this study, it has been observed that vulnerability exhibits a direct proportionality to the absence of adaptive capacity. These findings underscore that despite elevated levels of exposure and sensitivity, the overall susceptibility to extreme heat can be mitigated by enhancing adaptive capacity.

This study identified that the proportion of the area of high sensitivity index class within this study region was approximately 19% in 2021, whereas the figures observed in 2011 and 2016, were 27.44% and 27.68%, respectively. Particularly, in 2006, the prevalence of the area of very high sensitivity index class was considerably higher at 42.12%. Examining the dissemination area block size towards suburban and rural areas, farther from the regional core, reveals a comparatively larger block size, contributing to heightened percentage of sensitivity areas in the outer regions in 2006 (refer to Figure 4.1 for details). Additionally, when comparing the population centers of 2006 and 2011 to those of 2016 and 2021, a discernible shift is evident. In 2006 and 2011, the population distribution was dispersed, while in 2016 and 2021, it is notably concentrated toward the urban core. The size of the population center in 2006 and 2011 was 295 sq.km, while in

2016, it reduced to 248.57 sq.km, and in 2021, it measured 250 sq.km towards the urban core (see figure 4.7 for details). In the years following, a significant shift became apparent. By the year 2021, there was a notable increase in the elderly population, those aged 65 and above. Despite this rise in the proportion of elderly individuals within the population, their inclination towards residing in the regional core, combined with the smaller sizes of dissemination area blocks within this core area, led to a reduced percentage of the area classified under the heat-sensitivity index compared to data from 2006 and 2011. This transition suggests several key points:

a) The aging population, characterized by those aged 65 and above, experienced a noticeable increase over the years. This demographic trend is indicative of societal changes such as improved healthcare and increased life expectancy.
b) Elderly individuals showed a preference for living in the regional core. This could be due to factors such as access to amenities, healthcare facilities, social services, and transportation options which are typically more abundant in urban or regional core areas.
c) Within the regional core, the geographical units used for data analysis, known as dissemination area blocks, are smaller in size compared to other areas. This suggests a higher concentration of people in a smaller geographic area. Despite the increase in the elderly population and their concentration in the regional core, the proportion of the area classified as being sensitive to heat, as indicated by the heat-sensitivity index, has decreased when comparing the current data to data from earlier years, specifically 2006 and 2011. In 2006 and 2011, population concentration was more pronounced in the outer regions of the city, including

suburbs, and was more dispersed. In these areas, dissemination area blocks tended to be larger in size and occupied more extensive areas compared to those in the regional core. This dispersion and larger block sizes in the outer regions contributed to a higher percentage of the area being classified under the heat-sensitivity index during those years.

While the percentage of the area of very high sensitivity index class decreased, there was a concurrent twofold increase in the percentage of the area of high sensitivity index class, reaching 50.90% in 2021 compared to 25.06% in 2006. This shift is attributed to the effects of the influx of new elderly residents.

Surface temperature pertains to the actual temperature of the Earth's surface while air temperature denotes the temperature of the air approximately two meters above the ground. Land surfaces exhibit significant spatial variability, possess lower heat capacity, and have limited moisture content. In contrast, oceans exhibit homogeneity over vast scales, maintain nearly constant albedos, possess high heat capacity, and have an abundant moisture supply. On a sunny day, the temperature of the ground surface can exceed that of the air by more than 10 degrees Celsius (Utah State University, 2024). Additional research has shown temperature disparities ranging from 9 to 38 degrees Celsius (Naserikia et al., 2023).

Among the factors contributing to the calculation of UHI index values, albedo consistently exerts the most significant impact. Albedo denotes the portion of incoming sunlight (solar radiation) that a surface reflects. Urban elements like sidewalks, roads, buildings, and parking lots showcase low albedo, indicating their propensity to absorb more sunlight and emit it as heat into the urban environment. According to the global

map of local climate zones (LCZ) by (Demuzere et al., 2022), classes 1-10 correspond to the built environment. Investigation revealed that the population center (see figure 4.7 for reference) of Halifax is primarily characterized by built-up areas, predominantly falling into LCZ 5, 6, and 8 classes. LCZ 5 and LCZ 6 represent open midrise and open low rise, while LCZ 8 represents large low-rise classes, signifying a substantial presence of built environment (low albedo) and exhibits a notable deficiency in canopy cover in the population center. Previous research (Amindin et al., 2021; Schatz & Kucharik, 2014) highlighted that the built-up environment is a key factor contributing to the spatial changes in temperature patterns in urban areas. The presence of canopy cover has the potential to mitigate peak summer temperatures by 2-9°C in urban areas (Climate Central, 2023). Through a phenomenon known as evapotranspiration, plants play a role in cooling the air. A decrease in canopy cover corresponds to a reduction in evaporative cooling. Consequently, the population center, especially the regional core exhibits elevated values for LST, HVI and UHI. Conversely, suburbs areas mainly comprise of LCZ 11A, 12B, 13C, and LCZ 14D classes. Where LCZ 11 (A) is associated with dense trees, LCZ 12 (B) with scattered trees, LCZ 13 (C) with bush and scrub, and LCZ 14 (D) with low plants. Plants generally have higher albedo, resulting in lower HVI index values for suburban and rural areas.

To substantiate these findings, additional investigations was conducted and generated a distribution map of urban heat hotspots (Figure 4.7). As anticipated, this study observed that these hotspots are clustered exclusively within the population centers (refer to Figure 4.7 for more details), particularly concentrated in the urban core and exhibits very high density within the confines of the peninsula Halifax.

Even though the city is surrounded by coastal open water bodies, it is noteworthy that the regional core (i.e. peninsula, downtown Halifax, and Dartmouth) exhibits the highest UHI and HVI, UTFVI values, particularly in areas adjacent to water bodies (refer to figure 4.3, 4.8 and 4.9 for details). Notably, despite the presence of dense urban forests in certain areas (such as Point Pleasant Park, Africville Lookoff Park, Admiral Cove Park) surrounded by or adjacent to open water bodies, they fall within UHI classes characterized by very cold or cold temperatures. These findings reaffirm two crucial observations. Firstly, coastal, or open water bodies can notably contribute to the heightened UHI effect in urbanized areas. Secondly, regions with a dense urban forest or canopy cover can counteract the elevated UHI effect induced by coastal or open water bodies. In addition, insights from other studies (Steeneveld et al., 2014; van Hove et al., 2015) highlight that water bodies have a prolonged cooling process, potentially leading to warmer water bodies and amplifying Urban Heat Island effects.

From Table 4.3 and figure 4.9, it is evident that the highest percentages in the study area for all study years were categorized as either best (UTFVI <0) or worst (UTFVI > 0.020). Notably, Table 4.3 reveals that the intermediate categories had minimal percentages. The areas with the best thermal conditions (UTFVI < 0) were predominantly characterized by abundant canopy cover, primarily situated within suburban regions. These areas corresponded to LCZ 11 (A), associated with dense trees, LCZ 12 (B) with scattered trees, LCZ 13 (C) with bush and scrub, and LCZ 14 (D) with low plants. Previous research has indicated that these land uses typically fall within the best thermal zone (UTFVI <0) (Amindin et al., 2021; Portela et al., 2020). Conversely, the vast regions classified as the worst category mainly encompassed areas with scarce vegetation and built-up structures

(Amindin et al., 2021; Guha et al., 2018; Portela et al., 2020). This observation corresponds to results reported in previous studies conducted in two cities in Italy(Guha et al., 2018) and one city in Iran (Amindin et al., 2021), where it was noted that areas not affected by the UHI phenomenon showed little to no alteration in temperature, whereas regions affected by UHI experienced significant increases in heat stress. It is also observed that the regions exhibiting the worst (UTFVI) classifications correspondingly align with locales categorized as having very hot, hot, or temperate UHI conditions. None of the areas characterized by the worst UTFVI ratings were designated as cold or very cold. These findings are consistent with the literature (Amindin et al., 2021). When comparing with suburban areas the augmentation of impermeable surfaces and reduction of vegetation within urban settings has led to a heightened heat capacity and elevated thermal conductivity rates (Amindin et al., 2021; Oke, 1995; Song & Wang, 2015; Weng, 2001).

The HVI values reveal a discernible trend of elevated values within the inner urban core, including the downtown areas of both Halifax and Dartmouth, with a subsequent decrease extending towards suburban regions. Figure 4.10 illustrates the urban heat island surface profile, oriented from West to East (refer to figure 4.8) for all four study years, where the X and Y axes represent temperature (°C) and horizontal distance (meters), respectively. The regional center is situated within the range of 6000m to 15000m.

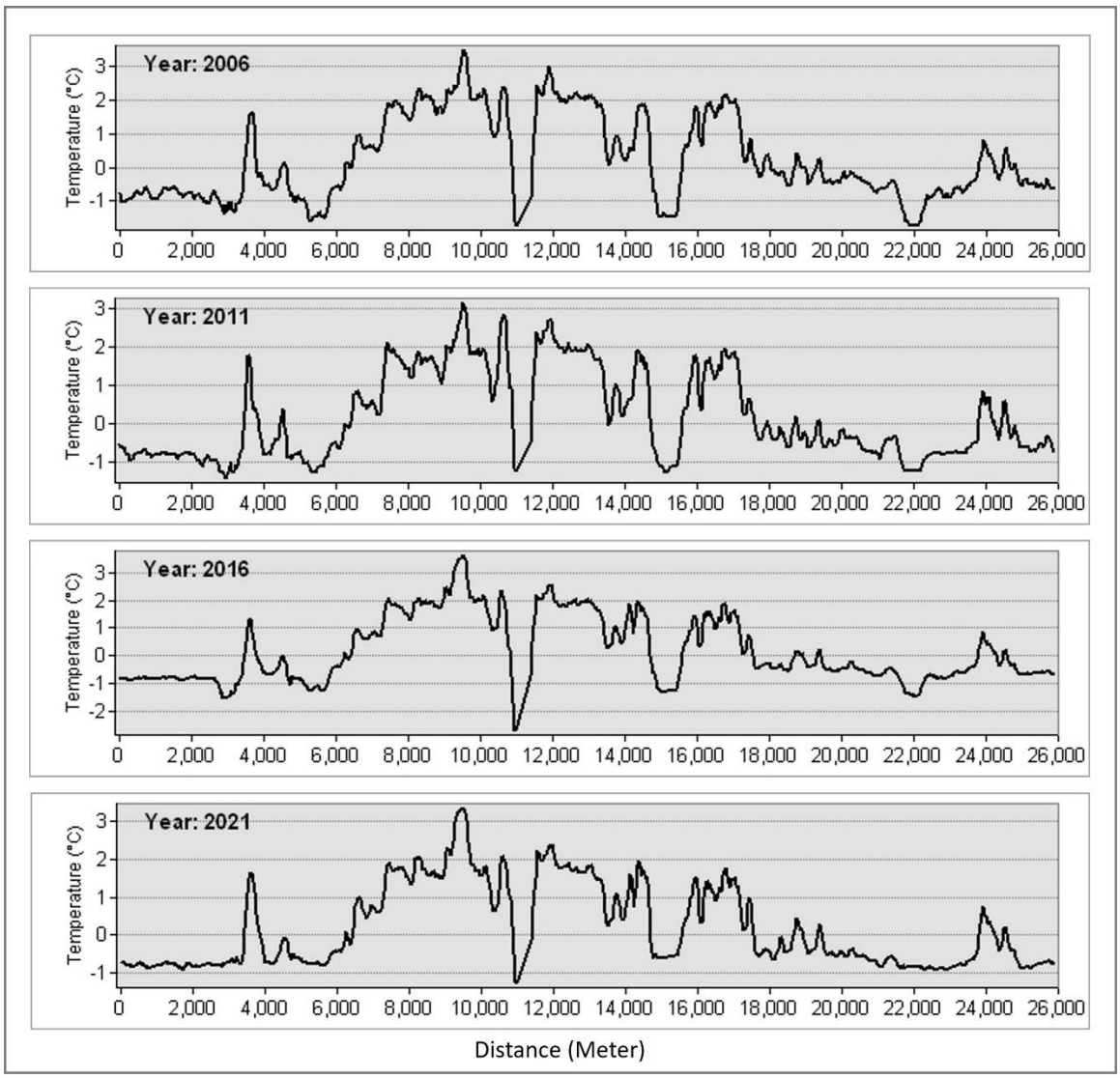

Figure 5.1, Temperature profile over the study area, with the formation of the UHI.

The figure clearly illustrates that moving away from the regional center (e.g., from 16000m to 26000m or 6000m to 0m) towards suburban areas is associated with a decline in temperature values. Notably, a substantial temperature drop is observed between 10000m and 12000m, attributed to the presence of the harbor between the peninsula and Darthmouth area.

The area characterized by elevated HVI exhibited an increase over time, with a constant dominance of very high heat exposure in the urban core of the study area from 2006 to

2016. In 2021, Very high heat exposed area was not limited to the urban core but also a substantial portion of the peninsula and Dartmouth transitioned from a high exposure class to a very high exposure class. Population density is crucial to explain this finding. The rise in population density and the expansion of residential land use intensifies urban heating (Amindin et al., 2021). In the context of a summer heat wave, the air conditioning systems in urban buildings can contribute an additional 20% of heat to the surrounding outdoor air (Climate Central, 2023). Data from Statistics Canada reveals the percentage change in population in Nova Scotia during the intervals 2006-2011, 2011-2016, and 2016-2021 to be 0.9%, 0.2%, and 5.0%, respectively (Statistics Canada, 2023). The marked 5% increase in population during the period from 2016 to 2021 emerges as a significant factor contributing to the elevated very high exposure index values observed in 2021. This provides clear evidence that population density plays a crucial role in influencing the obtained HVI. In conclusion, the very high heat vulnerable area in 2021 increased to 10.39% from 4.27% when compared to 2016.

Future growth areas (i.e., Future Growth Nodes) and special planning areas (i.e., SPAs) may have strong correlation with higher HVI. Core urban areas (e.g. Spryfield, Sackville, Port Wallace, Bedford) are exhibiting a trend of increasing HVI. This may have strong relationship with the future growth and development of the city as HRM and the province of NS has designated some areas as FGN and SPA (i.e. Bedford West 10, 12 and 1, Port Wallace, Dartmouth Crossing, former Penhorn Mall lands, Sandy Lake) (Halifax Regional Municipality, 2024). Since increased development will likely lead to higher LST, planners and other municipal agents should consider HVI in their reviews of development permits.

Government documents have been explaining several mitigation and adaptation measures. This study may assist decision makers to take decisions for future adaptation and mitigation plans. Among these endeavors, HalifACT stands out as one of the most ambitious climate action movements (Halifax Regional Municipalty, 2024). The unanimous adoption of HalifACT by the Halifax Regional Council on June 23, 2020, signifies a collaborative response to the climate crisis, with a specific focus on fostering resilience and improving the well-being of Atlantic Canada. This initiative is strategically oriented to address current climate challenges while proactively preparing for impending impacts. The overarching objective is to establish a robust and healthy trajectory for the region's sustainable development.

Chapter 5 of HalifACT provides a detailed overview of strategies focused on three main areas: creating sustainable and resilient infrastructure, fostering prepared and connected communities, and enhancing governance and leadership. These efforts are designed to meet climate targets from the present day to 2050. The chapter outlines various key actions, such as advocating for renewable energy, implementing eco-friendly government practices, preserving natural areas and green infrastructure, enhancing community readiness, conducting carbon assessments, and embedding climate considerations into municipal operations (Halifax Regional Municipalty, 2024).

Halifax Regional Municipality has taken proactive steps to promote climate-resilient construction practices, making both new and existing buildings more resilient to severe weather, flooding, and rising temperatures. The municipality aims to reduce greenhouse gas emissions by retrofitting existing structures and ensuring all new municipal buildings achieve net-zero emissions by 2030. Additionally, it is prioritizing the protection of water

resources against extreme weather events and refining wastewater management to reduce emissions.

In response to increasing heatwaves, the municipality has initiated a wide-ranging tree planting and greening program across the region. Naturalization efforts in parks and public areas not only combat urban heat islands but also improve water absorption. Climate considerations are being integrated into land use planning to enhance resilience and sustainability. Looking forward, the municipality is committed to engaging residents, raising awareness, and encouraging community participation in climate-resilient practices and responsibilities.

These identified actions align with the study findings, which underscore the significance of factors such as insufficient natural area, limited canopy cover, and diminished adaptive capacity as primary contributors to heightened heat vulnerability. The HalifACT initiative thus reinforces and complements the empirical outcomes of this study.

Chapter 6: Conclusions

This study identified a non-uniform pattern in the scores of the HVI between 2006 and 2021, indicating fluctuations rather than uniform growth. The HVI experienced periods of increase and decrease during this time frame, suggesting a dynamic pattern rather than a consistent upward trajectory. Nevertheless, a significant trend observed is the substantial increase seen in both the Very High and Very Low categories within the HVI for 2021. In the same year, Nova Scotia's population aged 65 years and older accounted for 22.2%, marking a 2.3 percentage point rise from 2016 (Statistics Canada, 2023). Furthermore, the 5% population surge between 2016 and 2021 collectively contributed significantly to the elevated very High HVI index values observed in 2021.

Throughout the preparation of the HVI, this study encountered several challenges. Firstly, the absence of health data prevented this study from measuring health-related sensitivity, resulted in to omit this aspect from this analysis. Additionally, due to the Landsat-8 satellite's 16-day repeat cycle, this study could only obtain two observations within any given one-month period. Obtaining cloud-free data for calculating Land Surface Temperature (LST) proved challenging, particularly this study focused on only two summer months (July and August). To address this issue, cloud masking techniques were applied to filter out cloudy pixels from the LST calculations. Furthermore, the unavailability of certain variables for all study years meant that this study was unable to include some useful variables in the analysis.

It's important to note that this study focused solely on land surface temperature-based heat vulnerability indexing. Factors such as air temperature, humidity levels, sunlight direction, and wind speed, which are typically crucial in measuring or indexing the disparity between actual and perceived temperatures, were not considered. This decision was made because our study aimed specifically at identifying heat-vulnerable areas resulting from land surface temperature in conjunction with socioeconomic and demographic factors.

A refined HVI would incorporate healthcare access, social isolation indicators, proximity to waterbodies, building age, building and road density among others to enhance its accuracy and effectiveness. Performing a more detailed spatial analysis like neighborhood level HVI would better serve the objective and will provide better insights to target interventions. Comparative analyses with other cities or regions would help to assess the transferability of the methodology and will be able to find out unique contextual factors influencing heat vulnerability. By addressing these future research opportunities, the study can contribute to advancing knowledge on urban heat vulnerability and resilience planning in Halifax. Finally, consideration of multiple years for heat vulnerability mapping to gain a comprehensive understanding of the trend and extent of vulnerable regions.

The concept of Heat Vulnerability Indexing (HVI) holds significant relevance for various stakeholders. Its utility extends to municipal governments where it serves as a crucial tool for decision-makers and urban planners. The framework employed in this study

represents a stride towards integrating the diverse factors influencing vulnerability across different scales. By incorporating these drivers of vulnerability, the HVI framework has the potential to empower communities and stakeholders to proactively develop mitigation strategies and effectively respond to heat-related emergencies. This contribution underscores the importance of adopting proactive measures to address heat vulnerability and underscores the significance of interdisciplinary collaboration in tackling this pressing issue.

References

Amindin, A., Pouyan, S., Pourghasemi, H. R., Yousefi, S., & Tiefenbacher, J. P. (2021). Spatial and temporal analysis of urban heat island using Landsat satellite images. *Environmental Science and Pollution Research*, *28*(30), 41439–41450. https://doi.org/10.1007/s11356-021-13693-0

Aminipouri, M., Knudby, A., & Ho, H. C. (2016). Using multiple disparate data sources to map heat vulnerability: Vancouver case study. *Canadian Geographer*, *60*(3), 356–368. https://doi.org/10.1111/cag.12282

Aubrecht, C., & Özceylan, D. (2013). Identification of heat risk patterns in the U.S. National Capital Region by integrating heat stress and related vulnerability. *Environment International*, *56*, 65–77. https://doi.org/10.1016/J.ENVINT.2013.03.005

Baccini, M., Kosatsky, T., Analitis, A., Anderson, H. R., D'Ovidio, M., Menne, B., Michelozzi, P., Biggeri, A., Kirchmayer, U., de'Donato, F., D'Ovidio, M., D'Ippoliti, D., Marino, C., McGregor, G., Accetta, G., Katsouyanni, K., Kassomenos, P., Sunyer, J., Atkinson, R., … Kalkstein, L. S. (2011). Impact of heat on mortality in 15 European cities: attributable deaths under different weather scenarios. *Journal of Epidemiology and Community Health*, *65*(1), 64–70. https://doi.org/10.1136/JECH.2008.085639

Bélanger, D., Gosselin, P., Valois, P., & Abdous, B. (2015). Neighbourhood and dwelling characteristics associated with the self-reported adverse health effects of heat in most deprived urban areas: A cross-sectional study in 9 cities. *Health & Place*, *32*,

8–18. https://doi.org/10.1016/J.HEALTHPLACE.2014.12.014

Beniston, M., Stephenson, D. B., Christensen, O. B., Ferro, C. A. T., Frei, C., Goyette, S., Halsnaes, K., Holt, T., Jylhä, K., Koffi, B., Palutikof, J., Schöll, R., Semmler, T., & Woth, K. (2007). Future extreme events in European climate: An exploration of regional climate model projections. *Climatic Change*, *81*(SUPPL. 1), 71–95. https://doi.org/10.1007/S10584-006-9226-Z/METRICS

Bradford, K., Abrahams, L., Hegglin, M., & Klima, K. (2015). A Heat Vulnerability Index and Adaptation Solutions for Pittsburgh, Pennsylvania. *Environmental Science and Technology*, *49*(19), 11303–11311. https://doi.org/10.1021/acs.est.5b03127

Brooke Anderson, G., & Bell, M. L. (2011). Heat waves in the United States: Mortality risk during heat waves and effect modification by heat wave characteristics in 43 U.S. communities. *Environmental Health Perspectives*, *119*(2), 210–218. https://doi.org/10.1289/ehp.1002313

Brooks, N., Adger, W. N., & Kelly, P. M. (2005). The determinants of vulnerability and adaptive capacity at the national level and the implications for adaptation. *Global Environmental Change*, *15*(2), 151–163. https://doi.org/10.1016/j.gloenvcha.2004.12.006

Canadian Red Cross. (2024). *Heat Waves : Information & Facts*. https://www.redcross.ca/how-we-help/emergencies-and-disasters-in-canada/types-of-emergencies/heat-waves/heat-waves-information-facts

Cardona, O. D., Van Aalst, M. K., Birkmann, J., Fordham, M., Mc Gregor, G., Rosa, P.,

Pulwarty, R. S., Schipper, E. L. F., Sinh, B. T., Décamps, H., Keim, M., Davis, I., Ebi, K. L., Lavell, A., Mechler, R., Murray, V., Pelling, M., Pohl, J., Smith, A. O., & Thomalla, F. (2012). Determinants of risk: Exposure and vulnerability. *Managing the Risks of Extreme Events and Disasters to Advance Climate Change Adaptation: Special Report of the Intergovernmental Panel on Climate Change*, *9781107025*, 65–108. https://doi.org/10.1017/CBO9781139177245.005

CCOHS. (2024). *Humidex rating and work*. Canadian Center for Occupational Health and Safety. https://www.ccohs.ca/oshanswers/phys_agents/humidex.html#section-1-hdr

Chauvin, F., & Denvil, S. (2007). Changes in severe indices as simulated by two French coupled global climate models. *Global and Planetary Change*, *57*(1–2), 96–117. https://doi.org/10.1016/J.GLOPLACHA.2006.11.028

Chow, W. T. L., Chuang, W. C., & Gober, P. (2012). Vulnerability to Extreme Heat in Metropolitan Phoenix: Spatial, Temporal, and Demographic Dimensions. *The Professional Geographer*, *64*(2), 286–302. https://doi.org/10.1080/00330124.2011.600225

Chow, W. T. L. L., Brennan, D., & Brazel, A. J. (2013). URBAN HEAT ISLAND RESEARCH IN PHOENIX, ARIZONA: Theoretical Contributions and Policy Applications. *American Meteorological Society*, *93*(4), 89. https://doi.org/10.1175/BAMS-D-11-00011.1

Chuang, W. C., & Gober, P. (2015). Predicting Hospitalization for Heat-Related Illness at the Census-Tract Level: Accuracy of a Generic Heat Vulnerability Index in Phoenix,

Arizona (USA). *Environmental Health Perspectives*, *123*(6), 606. https://doi.org/10.1289/EHP.1307868

Climate Central. (2023). *Urban Heat Hot Spots*. https://www.climatecentral.org/climate-matters/urban-heat-islands-2023

Coates, L., Haynes, K., O'Brien, J., McAneney, J., & De Oliveira, F. D. (2014). Exploring 167 years of vulnerability: An examination of extreme heat events in Australia 1844–2010. *Environmental Science & Policy*, *42*, 33–44. https://doi.org/10.1016/J.ENVSCI.2014.05.003

Cohen, S., Bush, E., Zhang, X., Nathan, G., Bonsal, B., Derksen, C., Flato, G., Greenan, B., & Watson, E. (2019). Synthesis of Findings for Canada's Regions. *Canada's Changing Climate*, 424–443.

Conlon, K. C., Mallen, E., Gronlund, C. J., Berrocal, V. J., Larsen, L., & O'neill, M. S. (2020). Mapping human vulnerability to extreme heat: A critical assessment of heat vulnerability indices created using principal components analysis. *Environmental Health Perspectives*, *128*(9), 1–14. https://doi.org/10.1289/EHP4030

Corbin, T. (2015). *Learning ArcGIS Pro 2*. Packt Publishing. https://www.google.ca/books/edition/Learning_ArcGIS_Pro/vDrlCwAAQBAJ?hl=en&gbpv=1&dq=Learning+ArcGIS+Pro+Corbin,+G.+T.+(2015)&printsec=frontcover

Demuzere, M., Kittner, J., Martilli, A., Mills, G., Moede, C., Stewart, I. D., Van Vliet, J., & Bechtel, B. (2022). A global map of local climate zones to support earth system modelling and urban-scale environmental science. *Earth System Science Data*,

14(8), 3835–3873. https://doi.org/10.5194/ESSD-14-3835-2022

Dietz, S., & Arnold, S. (2021). Atlantic Provinces; Chapter 1 in Canada in a Changing Climate: Regional Perspectives Report. In F.J. Warren, N. Lulham, & D.S. Lemmen (Eds.), *Chapter 1: Canada in a Changing Climate*. https://changingclimate.ca/site/assets/uploads/sites/4/2020/10/Atlantic-Provinces-Chapter-Regional-Perspectives-Report.pdf

Dong, W., Liu, Z., Zhang, L., Tang, Q., Liao, H., & Li, X. (2014). Assessing Heat Health Risk for Sustainability in Beijing's Urban Heat Island. *Sustainability 2014, Vol. 6, Pages 7334-7357*, *6*(10), 7334–7357. https://doi.org/10.3390/SU6107334

Downing, T. E., Patwardhan, A., Klein, R., Mukhala, E., Stephen, L., Winograd, M., & Ziervogel, G. (2005). *Assessing vulnerability for climate adaptation*. Cambridge University Press. https://hdl.handle.net/10568/55536

Environment and Climate Change Canada. (2023). *Environment and Climate Change Canada.* 1–31. https://wedocs.unep.org/bitstream/handle/20.500.11822/41263/Plastic_Science_E.pdf%0Ahttps://www.canada.ca/en/environment-climate-change/services/science-technology.html%0Ahttps://www.canada.ca/en/environment-climate-change/services/science-technology/cana

EPA - U.S. Environmental Protection Agency. (2012). *Heat Island Effect*. https://www.epa.gov/heatislands

Gaillard, J. C. (2010). Vulnerability, capacity and resilience: Perspectives for climate and development policy. *Journal of International Development*, *22*(2), 218–232.

https://doi.org/10.1002/JID.1675

Geladi, A. (2018). *Age-Friendly Built Environment: Examining the Downtown Core of the City of Kingston, Ontario*. *May*. https://qspace.library.queensu.ca/handle/1974/24257

Government of Canada. (2014). The Canadian Disaster Database. In *Public Safety Canada*. https://cdd.publicsafety.gc.ca/

Gronlund, C. J., Berrocal, V. J., White-Newsome, J. L., Conlon, K. C., & O'Neill, M. S. (2015). *Vulnerability to extreme heat by socio-demographic characteristics and area green space among the elderly in Michigan, 1990-2007*. *136*, 449–461. https://pubmed.ncbi.nlm.nih.gov/25460667/

Guha, S., Govil, H., Dey, A., & Gill, N. (2018). Analytical study of land surface temperature with NDVI and NDBI using Landsat 8 OLI and TIRS data in Florence and Naples city, Italy. *European Journal of Remote Sensing*, *51*(1), 667–678. https://doi.org/10.1080/22797254.2018.1474494

Guha, S., Govil, H., & Mukherjee, S. (2017). Dynamic analysis and ecological evaluation of urban heat islands in Raipur city, India. *Journal of Applied Remote Sensing*, *11*(03), 1. https://doi.org/10.1117/1.jrs.11.036020

Halifax regional municipality, 2000 International Pulp Bleaching Conference: Oral Presentations 7. Retrieved November 22, 2023, from https://www.halifax.ca/

Halifax Regional Municipality. (2024). *Special Planning Area*. Www.Halifax.Ca. https://www.halifax.ca/about-halifax/regional-community-planning/regional-

plan/special-planning-areas

Halifax Regional Municipalty. (2024). *HalifACT: Acting on Climate Together*. Www.Halifax.Ca. https://www.halifax.ca/about-halifax/energy-environment/halifact-2050-acting-climate-together

Harlan, S. L., Declet-Barreto, J. H., Stefanov, W. L., & Petitti, D. B. (2013). Neighborhood effects on heat deaths: Social and environmental predictors of vulnerability in Maricopa county, Arizona. *Environmental Health Perspectives*, *121*(2), 197–204. https://doi.org/10.1289/EHP.1104625/SUPPL_FILE/EHP.1104625.S001.PDF

Hasan, M. M., Islam, G. M. T., Matsumoto, P. S. S., Novak, M., & Rahaman, K. R. (2023). Employing Geographic Information Systems in Analyzing Pedestrian Accessibility to Public Bus Stops in Halifax. *Journal of Urban Planning and Development*, *149*(3), 04023016. https://doi.org/10.1061/JUPDDM.UPENG-4268

Health Canada. (2011). *Communicating the health risks of extreme heat events : toolkit for public health and emergency management officials*. http://www.hc-sc.gc.ca/ewh-semt/pubs/climat/heat-chaleur/index-eng.php#a1.0

Health Canada. (2023). *Health Canada*. https://www.canada.ca/en/health-canada.html

Health Canada, & Government of Canada. (2023). *Health Canada*. Encyclopedia of Nanoscience and Society. https://doi.org/10.4135/9781412972093.n161

Henderson, J. V., Nigmatulina, D., & Kriticos, S. (2021). Measuring urban economic density. *Journal of Urban Economics*, *125*, 103188.

https://doi.org/10.1016/J.JUE.2019.103188

Ho, H. C., Knudby, A., Walker, B. B., & Henderson, S. B. (2017). Delineation of spatial variability in the temperature-mortality relationship on extremely hot days in greater Vancouver, Canada. *Environmental Health Perspectives*, *125*(1), 66–75. https://doi.org/10.1289/EHP224

Hondula, D. M., Davis, R. E., Saha, M. V., Wegner, C. R., & Veazey, L. M. (2015). Geographic dimensions of heat-related mortality in seven U.S. cities. *Environmental Research*, *138*, 439–452. https://doi.org/10.1016/j.envres.2015.02.033

Huth, R., Kyselý, J., & Pokorná, L. (2000). A GCM simulation of heat waves, dry spells, and their relationships to circulation. *Climatic Change*, *46*(1–2), 29–60. https://doi.org/10.1023/A:1005633925903

Inostroza, L., Palme, M., & De La Barrera, F. (2016). A heat vulnerability index: Spatial patterns of exposure, sensitivity and adaptive capacity for Santiago de Chile. *PLoS ONE*, *11*(9), 1–26. https://doi.org/10.1371/journal.pone.0162464

IPCC. (2013). *AR5 Climate Change 2013: The Physical Science Basis — IPCC*. https://www.ipcc.ch/report/ar5/wg1/

Jalalzadeh Fard, B., Mahmood, R., Hayes, M., Rowe, C., Abadi, A. M., Shulski, M., Medcalf, S., Lookadoo, R., & Bell, J. E. (2021). Mapping Heat Vulnerability Index Based on Different Urbanization Levels in Nebraska, USA. *GeoHealth*, *5*(10), 1–18. https://doi.org/10.1029/2021GH000478

Jiménez-Muñoz, J. C., Sobrino, J. A., Plaza, A., Guanter, L., Moreno, J., & Martínez, P.

(2009). Comparison between fractional vegetation cover retrievals from vegetation indices and spectral mixture analysis: Case study of PROBA/CHRIS data over an agricultural area. *Sensors*, *9*(2), 768–793. https://doi.org/10.3390/s90200768

Johnson, D. P., Stanforth, A., Lulla, V., & Luber, G. (2012). Developing an applied extreme heat vulnerability index utilizing socioeconomic and environmental data. *Applied Geography*, *35*(1–2), 23–31. https://doi.org/10.1016/j.apgeog.2012.04.006

Karanja, J., & Kiage, L. (2021). Perspectives on spatial representation of urban heat vulnerability. *Science of the Total Environment*, *774*, 145634. https://doi.org/10.1016/j.scitotenv.2021.145634

Kennedy, M. S. (2021). Moving Forward Together. In *American Journal of Nursing* (Vol. 121, Issue 6, p. 7). https://doi.org/10.1097/01.NAJ.0000753572.44300.be

Kershaw, S. E., & Millward, A. A. (2012). A spatio-temporal index for heat vulnerability assessment. *Environmental Monitoring and Assessment*, *184*(12), 7329–7342. https://doi.org/10.1007/s10661-011-2502-z

Lemonsu, A., Viguié, V., Daniel, M., & Masson, V. (2015). Vulnerability to heat waves: Impact of urban expansion scenarios on urban heat island and heat stress in Paris (France). *Urban Climate*, *14*, 586–605. https://doi.org/10.1016/j.uclim.2015.10.007

Leya, R. S., Jodder, P. K., Rahaman, K. R., Chowdhury, M. A., Parida, D., & Islam, M. S. (2022). Spatial Variations of Urban Heat Island Development in Khulna City, Bangladesh: Implications for Urban Planning and Development. *Earth Systems and Environment*, *6*(4), 865–884. https://doi.org/10.1007/s41748-022-00309-x

Liu, L., & Zhang, Y. (2011). Urban Heat Island Analysis Using the Landsat TM Data and ASTER Data: A Case Study in Hong Kong. *Remote Sensing 2011, Vol. 3, Pages 1535-1552*, *3*(7), 1535–1552. https://doi.org/10.3390/RS3071535

Liu, X., Yue, W., Yang, X., Hu, K., Zhang, W., & Huang, M. (2020). Mapping Urban Heat Vulnerability of Extreme Heat in Hangzhou via Comparing Two Approaches. *Complexity*, *2020*. https://doi.org/10.1155/2020/9717658

Loughnan, M., Tapper, N. J., Phan, T., Lynch, K., & McInnes, J. (2013). A spatial vulnerability analysis of urban populations during extreme heat events in Australian capital cities. In *National Climate Change Adaptation Research Facility*. https://www.preventionweb.net/publication/spatial-vulnerability-analysis-urban-populations-during-extreme-heat-events-australian

Maier, G., Grundstein, A., Jang, W., Li, C., Naeher, L. P., & Shepherd, M. (2014). Assessing the Performance of a Vulnerability Index during Oppressive Heat across Georgia, United States. *Weather, Climate, and Society*, *6*(2), 253–263. https://doi.org/10.1175/WCAS-D-13-00037.1

Mallen, E., Stone, B., Lanza, K., Mallen, E., Stone, B., & Lanza, K. (2019). A methodological assessment of extreme heat mortality modeling and heat vulnerability mapping in Dallas, Texas. *Urban Climate*, *30*(February 2018), 100528. https://doi.org/10.1016/j.uclim.2019.100528

McGillivray, B. (2019). *Halifax. Encyclopedia Britannica*. https://www.britannica.com/place/Halifax-Nova-Scotia

Meehl, G. A., & Tebaldi, C. (2004). More intense, more frequent, and longer lasting heat

waves in the 21st century. *Science*, *305*(5686), 994–997. https://doi.org/10.1126/SCIENCE.1098704/SUPPL_FILE/MEEHL.SOM.PDF

Naheed, S., & Shooshtarian, S. (2021). A review of cultural background and thermal perceptions in urban environments. *Sustainability (Switzerland)*, *13*(16), 1–15. https://doi.org/10.3390/su13169080

Naim, M. N. H., & Kafy, A. Al. (2021). Assessment of urban thermal field variance index and defining the relationship between land cover and surface temperature in Chattogram city: A remote sensing and statistical approach. *Environmental Challenges*, *4*, 100107. https://doi.org/10.1016/j.envc.2021.100107

Naserikia, M., Hart, M. A., Nazarian, N., Bechtel, B., Lipson, M., & Nice, K. A. (2023). Land surface and air temperature dynamics: The role of urban form and seasonality. *Science of The Total Environment*, *905*, 167306. https://doi.org/10.1016/J.SCITOTENV.2023.167306

Nayak, S. G., Shrestha, S., Kinney, P. L., Ross, Z., Sheridan, S. C., Pantea, C. I., Hsu, W. H., Muscatiello, N., & Hwang, S. A. (2018). Development of a heat vulnerability index for New York State. *Public Health*, *161*, 127–137. https://doi.org/10.1016/j.puhe.2017.09.006

NOAA. (2023). *Assessing the Global Climate in April 2023 | News | National Centers for Environmental Information (NCEI)*. National Centers for Environmental Information. https://www.ncei.noaa.gov/news/global-climate-201912

NOAA. (2024). *Heat index*. National Oceanic and Atmospheric Administration. https://www.weather.gov/ama/heatindex

Office of Sustainability. (2023). *Heat Vulnerability Index Released by Multnomah County Health Department*. https://www.multco.us/sustainability/news/heat-vulnerability-index-released-multnomah-county-health-department

Oke, T. R. (1995). Wind Climate in Cities. *Wind Climate in Cities*, *December*. https://doi.org/10.1007/978-94-017-3686-2

Onozuka, D., & Hagihara, A. (2015). Variation in vulnerability to extreme-temperature-related mortality in Japan: A 40-year time-series analysis. *Environmental Research*, *140*, 177–184. https://doi.org/10.1016/J.ENVRES.2015.03.031

Philippe Roy, O., & David Huard, O. (2016). *FUTURE CLIMATE SCENARIOS PROVINCE OF NEW-BRUNSWICK* (Issue 9100). https://csrno.ca/climat/documents/Roy, Huard 2016 - Future Climate Scenarios Province.pdf

Portela, C. I., Massi, K. G., Rodrigues, T., & Alcântara, E. (2020). Impact of urban and industrial features on land surface temperature: Evidences from satellite thermal indices. *Sustainable Cities and Society*, *56*, 102100. https://doi.org/10.1016/J.SCS.2020.102100

Prihodko, L., & Goward, S. N. (1997). Estimation of air temperature from remotely sensed surface observations. *Remote Sensing of Environment*, *60*(3), 335–346. https://doi.org/10.1016/S0034-4257(96)00216-7

Rathi, S. K., Chakraborty, S., Mishra, S. K., Dutta, A., & Nanda, L. (2022). A heat vulnerability index: Spatial patterns of exposure, sensitivity and adaptive capacity for urbanites of four cities of india. *International Journal of Environmental*

Research and Public Health, *19*(1). https://doi.org/10.3390/ijerph19010283

Reid, C. E., O'Neill, M. S., Gronlund, C. J., Brines, S. J., Brown, D. G., Diez-Roux, A. V., & Schwartz, J. (2009). Mapping community determinants of heat vulnerability. *Environmental Health Perspectives*, *117*(11), 1730–1736. https://doi.org/10.1289/EHP.0900683/ASSET/62CE8B2A-F901-4E02-893E-51B032189A06/ASSETS/GRAPHIC/EHP-117-1730F2.JPG

Ren, H., Liu, R., Qin, Q., Fan, W., Yu, L., & Du, C. (2017). Mapping finer-resolution land surface emissivity using Landsat images in China. *Journal of Geophysical Research*, *122*(13), 6764–6781. https://doi.org/10.1002/2017JD026910

Renard, F., Alonso, L., Fitts, Y., Hadjiosif, A., & Comby, J. (2019). Evaluation of the effect of urban redevelopment on surface urban heat islands. *Remote Sensing*, *11*(3). https://doi.org/10.3390/RS11030299

Robine, J. M., Michel, J. P., & Herrmann, F. R. (2012). Excess male mortality and age-specific mortality trajectories under different mortality conditions: A lesson from the heat wave of summer 2003. *Mechanisms of Ageing and Development*, *133*(6), 378–386. https://doi.org/10.1016/j.mad.2012.04.004

Sabrin, S., Karimi, M., Fahad, M. G. R., & Nazari, R. (2020). Quantifying environmental and social vulnerability: Role of urban Heat Island and air quality, a case study of Camden, NJ. *Urban Climate*, *34*(August), 100699. https://doi.org/10.1016/j.uclim.2020.100699

Schär, C., Vidale, P. L., Lüthi, D., Frei, C., Häberli, C., Liniger, M. A., & Appenzeller, C. (2004). The role of increasing temperature variability in European summer

heatwaves. *Nature*, *427*(6972), 332–336. https://doi.org/10.1038/NATURE02300

Schatz, J., & Kucharik, C. J. (2014). Seasonality of the Urban Heat Island Effect in Madison, Wisconsin. *Journal of Applied Meteorology and Climatology*, *53*(10), 2371–2386. https://doi.org/10.1175/JAMC-D-14-0107.1

Sejati, A. W., Buchori, I., & Rudiarto, I. (2019). The spatio-temporal trends of urban growth and surface urban heat islands over two decades in the Semarang Metropolitan Region. *Sustainable Cities and Society*, *46*, 101432. https://doi.org/10.1016/J.SCS.2019.101432

Sheridan, S. C., Allen, M. J., Lee, C. C., & Kalkstein, L. S. (2012). Future heat vulnerability in California, Part II: Projecting future heat-related mortality. *Climatic Change*, *115*(2), 311–326. https://doi.org/10.1007/s10584-012-0437-1

Song, J., & Wang, Z. H. (2015). Interfacing the Urban Land–Atmosphere System Through Coupled Urban Canopy and Atmospheric Models. *Boundary-Layer Meteorology*, *154*(3), 427–448. https://doi.org/10.1007/s10546-014-9980-9

Stanforth, A. C., Johnson, D. P., Szagri, D., Nagy, B., Szalay, Z., Madrigano, J., Ito, K., Johnson, S., Kinney, P. L., Matte, T., Stanforth, A. C., & Johnson, D. P. (2016). Sociospatial Modeling for Climate-Based Emergencies: Extreme Heat Vulnerability Index. In *Urban Climate* (Vol. 52, Issue 7). https://doi.org/10.1007/978-3-319-30626-1_9

Statistics Canada. (2023). *Statistics Canada*. Government of Canada. https://www.statcan.gc.ca/en/start

Steeneveld, G. J., Koopmans, S., Heusinkveld, B. G., & Theeuwes, N. E. (2014). Refreshing the role of open water surfaces on mitigating the maximum urban heat island effect. *Landscape and Urban Planning*, *121*, 92–96. https://doi.org/10.1016/j.landurbplan.2013.09.001

Student, M. T., Kumar, R. R., Omments, R. E. C., Prajapati, A., Blockchain, T.-A., Ml, A. I., Randive, P. S. N., Chaudhari, S., Barde, S., Devices, E., Mittal, S., Schmidt, M. W. M., Id, S. N. A., PREISER, W. F. E., OSTROFF, E., Choudhary, R., Bit-cell, M., In, S. S., Fullfillment, P., … Fellowship, W. (2011). A "missing" family of classical orthogonal polynomials. *Journal of Physics A: Mathematical and Theoretical*, *44*(8), 1–13. https://doi.org/10.1088/1751-8113/44/8/085201

Sun, Q., Miao, C., Hanel, M., Borthwick, A. G. L., Duan, Q., Ji, D., & Li, H. (2019). Global heat stress on health, wildfires, and agricultural crops under different levels of climate warming. *Environment International*, *128*(April), 125–136. https://doi.org/10.1016/j.envint.2019.04.025

Tang, R., Li, Z. L., & Tang, B. (2010). An application of the Ts-VI triangle method with enhanced edges determination for evapotranspiration estimation from MODIS data in arid and semi-arid regions: Implementation and validation. *Remote Sensing of Environment*, *114*(3), 540–551. https://doi.org/10.1016/j.rse.2009.10.012

Tomlinson, C. J., Chapman, L., Thornes, J. E., & Baker, C. J. (2011a). Including the urban heat island in spatial heat health risk assessment strategies: A case study for Birmingham, UK. *International Journal of Health Geographics*, *10*(1), 1–14. https://doi.org/10.1186/1476-072X-10-42/FIGURES/9

Tomlinson, C. J., Chapman, L., Thornes, J. E., & Baker, C. J. (2011b). Including the urban heat island in spatial heat health risk assessment strategies: A case study for Birmingham, UK. *International Journal of Health Geographics*, *10*(1), 1–14. https://doi.org/10.1186/1476-072X-10-42/FIGURES/9

United States Environmental Protection Agency Office of Atmospheric Programs. (2006). Excessive Heat Events Guidebook. *Environmental Protection*, *June*, 60pp. https://scholar.google.com/scholar?q=EPA (Environmental Protection Agency) (2006). Excessive Heat Events Guidebook (1–60 Ed.). Washington%2C D.C.%2C Pennsylvania Avenue NW%3A United States Environmental Protection Agency.

Utah State University. (2024). *Surface Temperature*. Surface Temperature. https://doi.org/10.1515/9783035615111-009

van Hove, L. W. A., Jacobs, C. M. J., Heusinkveld, B. G., Elbers, J. A., Van Driel, B. L., & Holtslag, A. A. M. (2015). Temporal and spatial variability of urban heat island and thermal comfort within the Rotterdam agglomeration. *Building and Environment*, *83*, 91–103. https://doi.org/10.1016/j.buildenv.2014.08.029

Vautard, R., Yiou, P., D'Andrea, F., de Noblet, N., Viovy, N., Cassou, C., Polcher, J., Ciais, P., Kageyama, M., & Fan, Y. (2007). Summertime European heat and drought waves induced by wintertime Mediterranean rainfall deficit. *Geophysical Research Letters*, *34*(7), 1–5. https://doi.org/10.1029/2006GL028001

Vescovi, L., Rebetez, M., & Rong, F. (2005). Assessing public health risk due to extremely high temperature events: Climate and social parameters. *Climate Research*, *30*(1), 71–78. https://doi.org/10.3354/cr030071

Wang, F., Qin, Z., Song, C., Tu, L., Karnieli, A., & Zhao, S. (2015). An Improved Mono-Window Algorithm for Land Surface Temperature Retrieval from Landsat 8 Thermal Infrared Sensor Data. *Remote Sensing 2015, Vol. 7, Pages 4268-4289*, *7*(4), 4268–4289. https://doi.org/10.3390/RS70404268

Wang, H., Zhang, Y., Tsou, J. Y., & Li, Y. (2017). Surface Urban Heat Island Analysis of Shanghai (China) Based on the Change of Land Use and Land Cover. *Sustainability 2017, Vol. 9, Page 1538*, *9*(9), 1538. https://doi.org/10.3390/SU9091538

Weng, Q. (2001). A remote sensing?GIS evaluation of urban expansion and its impact on surface temperature in the Zhujiang Delta, China. *International Journal of Remote Sensing*, *22*(10), 1999–2014. https://doi.org/10.1080/713860788

WMO. (2019). *United in Science | 1 | World Meteorological Organization*. https://wmo.int/publication-series/united-science

Wolf, T., & McGregor, G. (2013). The development of a heat wave vulnerability index for London, United Kingdom. *Weather and Climate Extremes*, *1*, 59–68. https://doi.org/10.1016/J.WACE.2013.07.004

World Bank. (2024). *United Arab Emirates*. Climate Change Knowledge Portal. https://climateknowledgeportal.worldbank.org/country/united-arab-emirates/climate-data-historical#:~:text=The summer season (June to,C to 37.2°C.

Xu, L. Y., Xie, X. D., & Li, S. (2013). Correlation analysis of the urban heat island effect and the spatial and temporal distribution of atmospheric particulates using TM images in Beijing. *Environmental Pollution*, *178*, 102–114.

https://doi.org/10.1016/J.ENVPOL.2013.03.006

Yang, L., Qian, F., Song, D. X., & Zheng, K. J. (2016). Research on Urban Heat-Island Effect. *Procedia Engineering*, *169*, 11–18. https://doi.org/10.1016/j.proeng.2016.10.002

Yuan, F., & Bauer, M. E. (2007). Comparison of impervious surface area and normalized difference vegetation index as indicators of surface urban heat island effects in Landsat imagery. *Remote Sensing of Environment*, *106*(3), 375–386. https://doi.org/10.1016/J.RSE.2006.09.003

Zhang, Y., Yu Tao, X. fa G., Yu-xiang, Z., Yu, S., Zhang, W., & Li, X. (2006). Land Surface Temperature Retrieval from CBERS-02 IRMSS Thermal Infrared Data and Its Applications in Quantitative Analysis of Urban Heat Island Effect. *National Remote Sensing Bulletin*, *0*(5), 789–797. https://doi.org/10.11834/jrs.200605117

Appendix A

Year 2006: Z – Score

Population Density	LST	Built-up area	Canopy Cover	Male Population	Very Young Population	Elderly Population	Living alone	Private HHs rented	Population with No knowledge of official language	Non-Canadian Population living in private HHs	Population over 15 years old with no fixed workplace	Population over 15 years old with no private car	Population over 15 years old without high school degree	Ethnicity	Low Income HHs
0.284	0.023	0.665	0.517	0.070	0.260	0.827	0.001	0.381	0.186	1.805	0.743	0.888	0.777	0.761	0.127
0.284	0.409	0.665	0.517	0.294	1.201	0.456	1.223	1.115	0.186	0.603	1.632	0.319	0.035	0.760	0.644
0.012	0.303	0.665	0.517	0.070	0.681	0.473	0.659	0.604	0.186	0.603	0.536	0.699	0.574	0.665	0.644
0.433	0.826	0.665	0.517	0.740	1.622	0.659	0.659	1.115	0.186	0.603	1.632	1.363	0.979	0.191	0.644
0.266	0.265	0.436	0.226	0.153	0.260	0.473	1.035	1.115	0.186	1.324	1.084	1.078	0.137	0.190	0.313
0.044	0.007	0.665	0.517	0.070	0.681	0.270	0.093	0.161	0.186	0.603	0.926	0.509	0.137	0.096	0.238
0.412	0.260	0.511	0.405	1.046	0.210	0.473	0.753	0.668	0.186	0.362	0.012	0.983	0.371	0.380	0.644
0.440	0.376	0.665	0.517	0.740	0.210	0.270	0.282	0.254	0.186	0.362	0.536	0.060	0.066	0.475	0.423
0.469	0.635	0.530	0.517	0.153	0.260	3.056	0.471	0.289	0.186	0.603	0.536	1.078	0.979	0.760	0.238
0.463	0.465	0.665	0.517	0.740	0.681	0.845	0.095	0.030	0.186	0.603	0.012	0.414	0.543	0.570	1.009
0.401	0.514	0.659	0.517	0.376	0.260	0.845	0.847	1.115	0.186	0.360	1.632	0.983	0.675	0.095	0.644
0.728	1.843	1.887	2.510	0.823	0.731	1.030	0.753	1.115	0.186	0.119	1.084	0.841	0.574	0.285	0.644
0.373	0.322	0.074	0.227	1.046	0.260	0.270	1.129	0.987	0.186	0.603	0.353	0.888	0.777	0.475	0.423
0.426	0.303	0.665	0.517	0.740	0.681	0.641	0.565	0.317	0.186	0.603	0.743	0.487	0.574	0.380	0.017
0.674	1.292	0.639	0.995	0.153	0.210	0.102	0.753	0.445	0.186	0.121	0.170	0.604	0.777	0.286	0.534
0.633	1.533	0.838	0.528	0.376	0.210	0.084	0.847	1.115	0.186	0.603	0.012	0.983	0.878	0.475	0.644
0.713	1.818	1.481	1.375	0.376	1.622	0.084	0.941	0.732	0.186	0.119	0.170	0.983	0.574	0.001	0.313
0.170	0.752	0.097	0.118	0.600	1.151	0.287	1.129	1.115	0.186	0.603	0.901	0.651	0.777	0.285	0.644
0.716	1.116	0.665	0.517	0.963	0.210	1.402	0.376	0.923	0.186	0.119	0.901	0.793	0.777	0.760	0.644
0.085	0.615	0.665	0.517	0.070	0.260	0.102	0.847	1.115	0.186	0.603	0.170	0.556	0.168	0.190	0.423
0.130	0.301	0.514	0.264	0.823	0.260	0.102	0.941	0.987	0.186	0.603	0.719	0.699	0.878	0.760	0.644
0.020	0.220	0.555	1.528	0.740	2.093	0.270	0.095	1.054	0.186	0.603	0.353	0.298	1.456	1.332	0.348
0.182	0.447	0.649	0.491	0.376	0.260	1.013	1.223	1.115	0.186	0.603	1.632	0.461	0.777	0.571	0.644
0.235	0.776	0.665	0.517	0.070	0.260	1.570	0.282	0.955	0.186	0.603	0.378	0.556	0.066	0.095	0.644
0.447	0.685	0.665	0.517	0.070	0.260	0.827	0.093	0.030	0.186	0.360	0.353	0.556	0.066	0.380	0.093

Year 2011: Z – Score															
Population Density	LST	Built-up area	Canopy Cover	Male Population	Very Young Population	Elderly Population	Living alone	Private HHs rented	Population with No knowledge of official language	Non-Canadian Population living in private HHs	Population over 15 years old with no fixed workplace	Population over 15 years old with no private car	Population over 15 years old without high school degree	Ethnicity	Low Income HHs
0.206	0.867	0.154	0.664	0.112	0.058	0.284	0.151	0.330	0.426	0.484	0.448	0.294	1.039	0.509	0.337
0.419	0.444	0.880	0.664	0.062	1.396	0.627	0.619	0.152	2.477	0.484	0.160	1.283	0.765	0.027	0.207
0.732	1.942	1.633	1.907	0.412	0.950	0.106	0.785	1.053	0.426	0.484	1.298	0.944	0.673	0.751	0.989
0.616	1.473	1.650	2.975	0.412	0.388	0.236	0.878	1.053	0.426	0.271	1.177	1.268	0.151	0.590	0.793
0.133	0.847	1.161	2.346	0.062	1.396	0.367	0.504	1.053	0.426	0.484	1.420	0.897	1.616	0.751	0.184
0.251	0.784	0.136	0.001	0.112	1.842	0.497	0.245	1.958	0.426	0.120	0.326	1.005	3.081	2.145	3.117
0.032	1.666	2.212	1.675	0.412	2.288	1.018	0.878	0.782	0.426	0.484	0.205	1.315	0.673	0.751	0.467
0.434	0.174	0.415	0.419	1.112	0.950	0.887	0.713	1.356	3.929	0.484	1.055	0.726	1.799	0.778	0.640
0.551	0.904	0.880	0.664	0.062	3.180	0.887	0.317	1.838	0.426	0.484	1.011	0.031	2.073	2.467	2.726
0.004	0.888	0.880	0.664	0.587	0.058	0.367	0.806	0.694	0.426	0.484	0.326	0.170	0.242	0.268	0.510
0.483	0.692	0.967	1.443	0.237	0.058	0.154	0.410	1.477	0.426	0.182	0.281	0.851	1.223	0.027	0.836
0.203	0.291	0.646	0.643	8.330	2.173	1.668	1.253	0.511	0.426	0.484	1.011	2.164	1.406	0.751	0.402
0.039	0.229	0.332	0.041	0.462	0.388	0.935	0.619	0.481	0.426	0.484	0.205	0.665	0.059	0.751	0.532
1.189	0.022	0.859	0.425	0.287	0.388	0.887	0.245	0.752	0.426	0.484	1.011	0.619	0.399	0.348	0.989
0.135	0.248	0.535	0.209	0.587	0.504	0.414	0.785	0.932	0.426	0.484	0.083	1.129	0.948	0.188	0.728
0.748	0.107	0.585	0.349	0.762	2.288	0.154	0.597	1.687	2.477	1.478	0.812	2.211	1.406	0.134	0.337
0.187	0.821	1.186	2.004	0.412	0.058	0.757	0.878	0.212	0.426	2.987	0.448	0.897	1.039	1.743	0.207
0.466	1.109	1.390	0.740	0.637	1.727	4.190	0.058	0.302	0.426	0.031	0.160	0.341	0.673	0.268	0.728
2.453	1.696	0.744	0.664	0.412	1.281	0.887	1.649	1.326	0.426	2.383	0.524	2.257	1.039	1.421	2.530
0.030	0.594	0.579	0.664	0.062	0.388	0.887	1.065	1.053	0.426	0.484	0.326	0.897	0.582	0.375	0.142
0.778	0.761	0.717	0.655	0.412	1.842	1.408	0.785	1.053	0.426	0.484	1.011	0.758	0.242	0.751	0.989
0.237	1.607	2.135	1.393	0.637	0.058	1.326	0.151	1.053	0.426	1.025	0.403	1.036	0.673	0.456	0.207
0.480	0.768	0.753	0.632	0.287	0.058	0.675	0.806	0.332	5.381	0.182	0.524	0.016	1.406	0.348	0.402
0.661	0.263	0.254	0.135	1.686	0.834	3.279	1.836	0.182	0.426	0.484	0.569	0.355	1.406	0.134	0.272
0.892	0.551	0.197	0.561	0.462	0.834	0.154	1.555	1.868	0.426	2.383	0.569	0.201	1.158	1.663	1.422
0.604	1.236	0.535	0.549	0.462	0.834	1.456	0.713	1.838	0.426	0.422	0.160	0.170	0.215	0.027	0.575

Year 2016: Z – Score															
Population Density	LST	Built-up area	Canopy Cover	Male Population	Very Young Population	Elderly Population	Living alone	Private HHs rented	Population with No knowledge of official language	Non-Canadian Population living in private HHs	Population over 15 years old with no fixed workplace	Population over 15 years old with no private car	Population over 15 years old without high school degree	Ethnicity	Low Income HHs
0.38	1.16	0.58	0.51	0.25	0.20	0.93	0.46	0.91	0.31	1.27	1.48	0.75	0.06	0.08	0.49
0.21	0.46	0.58	0.51	0.28	0.20	0.68	1.56	1.23	0.31	0.19	0.83	1.06	0.30	0.25	1.01
0.75	2.14	2.51	0.51	0.52	0.20	0.19	1.04	0.94	0.31	0.55	0.90	0.24	0.55	0.77	0.78
0.35	0.20	0.58	0.51	0.02	0.76	0.06	1.69	0.97	0.31	0.44	0.25	0.65	1.04	0.10	1.01
0.72	0.77	0.58	0.39	1.05	0.68	0.80	1.93	1.80	0.28	1.27	3.21	0.67	2.75	0.71	3.50
0.70	1.48	0.73	0.51	0.28	0.28	0.06	0.65	0.46	0.31	0.08	0.64	1.00	0.43	0.86	0.71
0.49	0.48	0.56	0.19	0.55	1.65	0.06	0.52	0.24	0.31	0.17	0.45	0.95	0.80	0.51	0.04
0.66	1.45	2.20	0.51	1.05	0.76	0.06	0.98	1.07	0.31	0.64	0.64	0.65	1.04	0.77	0.49
0.01	0.31	0.58	0.51	0.78	1.65	0.18	0.77	1.80	5.65	1.33	0.83	0.87	1.04	3.49	2.84
0.41	1.24	0.58	0.51	0.02	0.20	0.68	1.54	1.96	0.31	0.19	1.29	0.16	0.43	0.36	1.14
0.11	0.02	0.58	0.51	0.52	1.24	0.31	0.65	0.46	0.31	1.42	1.22	1.48	1.04	0.42	0.56
0.10	0.27	0.58	2.85	0.25	0.76	0.31	0.72	0.91	0.31	0.62	0.06	0.04	0.79	0.86	0.78
0.28	1.09	0.58	0.41	0.25	0.28	0.06	0.57	1.16	0.31	0.62	1.41	1.07	1.04	0.71	0.10
0.07	0.76	0.58	0.51	0.25	0.28	0.18	1.23	1.23	0.31	0.91	1.22	0.85	1.16	0.77	0.78
0.13	0.54	0.58	1.23	0.82	0.68	0.19	0.46	0.43	0.31	0.82	1.22	0.85	0.06	0.77	0.41
0.43	0.43	0.04	0.18	0.25	0.76	1.17	0.65	1.00	0.31	1.18	0.32	0.40	0.06	1.03	0.71
0.81	1.81	2.54	2.67	0.52	0.76	0.19	0.98	1.07	0.31	0.26	0.71	1.00	0.18	0.51	0.86
0.37	0.97	0.58	0.51	0.55	1.17	0.19	0.32	0.34	0.28	1.09	0.13	0.04	1.16	0.01	0.92
0.05	0.31	0.58	0.51	0.25	0.68	0.18	0.25	0.11	0.31	1.33	0.06	1.28	1.16	0.77	0.27
0.88	1.02	0.58	0.51	0.28	0.28	0.68	0.14	0.30	0.31	0.26	0.25	1.58	0.06	0.68	0.27
0.33	1.33	1.42	0.51	0.25	0.20	0.92	1.36	1.07	0.31	0.37	1.09	1.16	0.55	0.16	0.93
0.20	0.23	0.58	0.64	1.05	0.20	0.31	0.57	0.08	0.31	1.36	0.71	0.04	1.16	0.10	0.47
0.50	0.70	0.58	0.51	0.78	0.28	0.31	0.20	0.30	0.31	0.35	1.02	0.45	1.04	0.16	0.56
0.18	0.24	0.58	0.51	0.55	0.68	0.31	0.59	0.05	0.28	0.17	2.25	0.95	0.18	0.19	0.19
0.22	0.63	0.58	0.33	0.52	0.76	0.31	0.90	0.34	0.31	1.06	0.25	0.11	0.55	0.68	0.49
0.63	1.35	0.58	0.51	0.25	1.24	0.06	1.29	1.20	0.31	1.51	1.22	1.73	1.53	0.53	0.40

Year 2021: Z – Score															
Population Density	LST	Built-up area	Canopy Cover	Male Population	Very Young Population	Elderly Population	Living alone	Private HHs rented	Population with No knowledge of official language	Non-Canadian Population living in private HHs	Population over 15 years old with no fixed workplace	Population over 15 years old with no private car	Population over 15 years old without high school degree	Ethnicity	Low Income HHs
0.30	0.11	0.01	0.64	0.37	0.39	0.95	0.29	0.39	0.44	1.04	0.80	1.14	1.11	0.66	0.57
0.25	0.06	0.61	1.06	0.34	1.50	0.29	1.19	1.28	0.44	0.53	1.84	0.89	0.72	1.15	1.29
0.11	0.09	0.36	1.00	0.14	0.39	0.05	0.84	0.70	0.44	1.00	0.14	0.95	0.85	0.80	0.57
0.45	0.52	1.09	0.35	1.08	1.50	1.27	0.91	1.28	2.99	2.10	1.84	1.45	0.72	0.52	0.25
0.29	0.53	0.56	0.51	0.34	0.39	0.27	1.67	1.28	0.44	0.53	1.84	2.08	0.72	0.10	0.62
0.08	0.24	0.79	1.43	0.19	0.39	0.38	0.67	0.22	0.42	0.73	0.47	0.51	0.33	0.59	0.04
0.30	0.32	0.37	0.79	0.20	0.95	0.38	0.84	0.48	0.44	0.37	0.52	0.95	0.33	0.10	0.33
0.43	0.27	0.24	0.18	0.30	0.17	0.51	0.40	0.13	0.44	0.06	0.69	0.95	0.58	0.38	0.06
0.49	0.68	0.55	0.88	0.48	1.28	1.73	0.67	0.04	0.42	0.89	0.52	0.39	0.07	1.15	0.33
0.42	0.68	0.98	1.38	0.54	0.17	0.51	0.57	0.16	0.44	0.10	0.96	0.51	0.46	0.94	0.49
0.43	0.80	0.88	1.37	0.53	0.17	0.73	0.91	1.12	0.42	1.00	0.36	0.51	0.46	0.17	0.42
0.70	1.62	1.22	1.32	0.79	0.72	0.27	0.91	1.28	0.44	0.84	0.03	2.08	0.46	0.31	0.42
0.42	0.48	0.49	1.05	0.60	1.28	0.05	1.32	0.93	0.44	0.06	1.84	1.33	0.59	0.80	0.81
0.42	0.16	0.42	0.13	0.47	0.39	0.38	0.12	0.03	0.44	0.84	1.45	0.33	0.20	0.73	0.33
0.66	0.59	0.34	0.26	0.29	0.95	0.38	0.64	0.51	0.42	0.69	0.19	0.45	0.46	0.04	0.38
0.58	1.28	1.08	0.02	0.34	0.72	0.17	0.84	1.21	0.42	0.10	0.36	0.64	0.07	0.73	0.91
0.68	1.70	1.26	0.93	0.29	0.39	0.60	1.12	0.93	0.44	0.10	1.02	0.70	0.72	0.38	0.42
0.22	0.46	0.11	0.48	0.32	0.39	0.16	1.53	1.28	0.42	0.53	0.52	1.01	0.07	0.52	0.95
0.48	0.96	1.65	0.88	1.18	0.17	0.16	0.81	0.51	0.44	0.69	0.30	0.83	0.46	0.31	0.47
0.04	0.32	0.04	0.22	0.02	0.95	0.27	0.98	1.15	0.42	0.69	0.69	0.45	0.20	0.73	0.57
0.18	0.05	0.23	0.86	0.57	0.17	0.29	0.98	1.15	0.44	0.37	0.14	0.70	0.59	0.31	0.57
0.04	0.20	0.23	0.15	0.52	0.17	0.83	0.15	0.92	0.44	0.73	0.47	1.61	0.45	1.50	0.73
0.25	0.27	0.30	0.58	0.07	0.17	0.62	0.77	1.28	0.44	1.52	1.84	1.58	0.46	0.04	1.10
0.24	0.55	0.54	0.03	0.58	1.28	0.40	0.08	1.28	0.44	4.35	0.96	0.05	0.58	0.31	0.66
0.38	0.57	0.65	0.54	0.41	0.72	0.29	0.33	0.03	0.44	0.37	1.29	0.61	0.71	0.38	0.42
0.45	0.49	0.29	0.79	0.03	1.28	0.95	0.15	0.42	0.44	0.41	0.63	0.33	1.89	0.73	0.71